TABLE 1. Primer and probe sequences for real-time PCR analysis for preproghrelin, GH, GHRH, somatostatin, and GHS-R mRNAs

	Primer and probe sequences
Preproghrelin	
Forward	5′-GCATGCTCTGGATGGACATG-3′
Reverse	5′-TGGTGGCTTCTTGGATTCCT-3′
Probe	5′-AGCCCAGAGCACCAGAAAGCCCA-3′
GH	
Forward	5′-AAGAGTTCGAGCGTGCCTACA-3′
Reverse	5′-GAAGCAATTCCATGTCGGTTC-3′
Probe	5′-CCATTCAGAATGCCCAGGCTGCTTTC-3′
GHRH	
Forward	5′-AGGATGCAGCGACACGTAGA-3′
Reverse	5′-TCTCCCCTTGCTTGTTCATGA-3′
Probe	5′-CCACCAACTACAGGAAACTCCTGAGCCA-3′
Somatostatin	
Forward	5′-AGCTGAGCAGGACGAGATGAG-3′
Reverse	5′-ACAGGATGTGAATGTCTTCCAGAA-3′
Probe	5′-CGAACCCAGCAATGGCACCCC-3′
GHS-R	
Forward	5′-CACCAACCTCTACCTATCCAGCAT-3′
Reverse	5′-CTGACAAACTGGAAGAGTTTGCA-3′
Probe	5′-TAAGATCTGCTCATCTTAATGTGCATG-3′

minipumps were implanted into the peritoneum. Des-acyl ghrelin or saline was infused continuously through the minipumps into 4-wk-old C57/BL6 mice (Japan CLEA) for 10 d. The minipumps were continuously delivering saline or 250 μg/kg·d of des-acyl ghrelin for 10 d at a speed of 0.22 μl/h. Body weights were measured daily for 10 d. Four hundred microliters of blood samples for the measurement of serum GH and IGF-1 levels were collected from the inferior vena cava of mice under anesthesia with diethyl ether 10 d after the implantation.

Hematoxylin eosin and immunohistochemical staining for total ghrelin, acylated ghrelin, and GH of the pituitary

The pituitaries were removed from male 8-wk-old mice under anesthesia with diethyl ether and fixed with 4% paraformaldehyde and 0.2% picric acid and embedded in paraffin. The tissues were cut in 3-μm-thick slices. Samples were subjected to immunohistochemical staining for total and acylated ghrelin as well as hematoxylin eosin staining. After pretreatment with 0.3% hydrogen peroxide and incubation with normal goat serum, all slices were incubated overnight at 4 C with ghrelin(13–28) antiserum recognizing total (des-acyl plus acylated) ghrelin (final dilution, 1:5000), antighrelin(1–11) antiserum specifically recognizing acylated ghrelin (final dilution, 1:5000), or anti-GH antiserum (Biogenesis, Poole, UK) (final dilution, 1:200). All of the sections were stained by the avidin-biotin complex method and counterstained with hematoxylin as reported previously (39).

Statistical analysis

Results are expressed as the mean ± SEM. ANOVA followed by the *t* test was used to assess differences between control and transgenic mice. $P < 0.05$ was considered to be statistically significant.

Results

Generation of transgenic mice and preproghrelin mRNA levels

Two lines of transgenic mice with six (Tg 10–1) and 12 (Tg 9–2) copy numbers were identified by PCR and Southern blot analysis. Preproghrelin mRNAs were detected only in the stomach, small intestine, lung, pituitary, and hypothalamus of control mice, and the amounts were 100, 4, 2.1, 1.5, and 0.5 in arbitrary units (AU), respectively (Fig. 1). On the other hand, they were detected in all tissues examined in Tg 9–2 and Tg 10–1 mice, and the amounts in the stomach of Tg 9–2 and Tg 10–1 mice reached 1100 and 5200 AU, respectively (Fig. 1). Preproghrelin mRNA levels in other tissues of Tg 9–2 and Tg 10–1 mice also exceeded those of control mice.

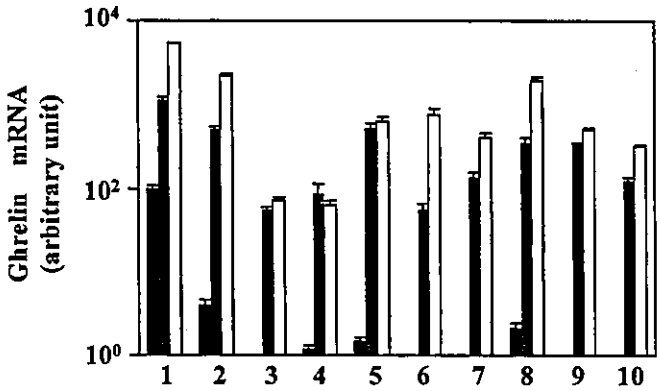

FIG. 1. Preproghrelin mRNA levels in the tissues of control (*closed bars*), Tg 9–2 (*shaded bars*), and Tg 10–1 (*open bars*) mice quantified by real-time PCR analysis. Lanes 1, stomach; 2, small intestine; 3, cerebrum; 4, hypothalamus; 5, pituitary; 6, liver; 7, kidney; 8, lung; 9, heart; and 10, skeletal muscle.

Total and acylated ghrelin levels in tissues and plasma

Eight-week-old control, Tg 9–2, and Tg 10–1 mice were used (Table 2). Although high total ghrelin levels were detected in the stomach, only very low levels were detected in other tissues of control mice. Tg 9–2 and Tg 10–1 mice showed significantly higher total ghrelin levels in the stomach than control mice ($P < 0.01$ for each). Tg 9–2 and Tg 10–1 mice also showed total ghrelin levels in all of the other tissues significantly higher than control mice. High levels of acylated ghrelin were also detected in the stomach of control, Tg 9–2, and Tg 10–1 mice. There was, however, no significant difference between control and Tg 9–2 mice and between control and Tg 10–1 mice. Only very low acylated ghrelin levels if any were detected in other tissues of control, Tg 9–2, and Tg 10–1 mice. Plasma total ghrelin levels in control, Tg 9–2, and Tg 10–1 mice were 1104.5 ± 94.4, 11230.6 ± 1147.1, and 48565.5 ± 9291.5 fmol/ml, respectively. Those in Tg 9–2 and Tg 10–1 mice were significantly higher than those in control mice ($P < 0.01$ for each). Plasma acylated ghrelin levels in control, Tg 9–2, and Tg 10–1 mice were 83.7 ± 11.9, 79.7 ± 10.1, and 86.3 ± 21.1 fmol/ml, respectively. The differences between control and Tg 9–2 mice and control and Tg 10–1 mice were not significant.

Body weights and lengths, relative organ weights, and BMIs

Body weights of control, Tg 9–2, and Tg 10–1 mice are shown in Table 3 and Fig. 2A. Male Tg 9–2 and Tg 10–1 mice were significantly lighter in the body weight than control mice ($P < 0.05$ and $P < 0.01$, respectively). Female Tg 10–1 mice were also significantly lighter than control mice ($P < 0.01$). The difference between female control and Tg 9–2 mice was not significant. Fifteen-week-old male and female Tg 10–1 and male Tg 9–2 mice were still significantly lighter than control mice ($P < 0.05$, $P < 0.01$, and $P < 0.01$, respectively). Body lengths (nose-to-anus lengths) of control and

TABLE 2. Total and acylated ghrelin levels in plasma and tissues of 8-wk-old control and transgenic mice (n = 8/group)

	Control	Tg 9-2	Tg 10-1
Total ghrelin			
Plasma (fmol/ml)	1104.5 ± 94.4	11230.6 ± 1147.1[a]	48565.5 ± 9291.5[a]
Tissues (fmol/mg)			
Stomach	2191.9 ± 340.9	2860.8 ± 587.3[a]	5430.6 ± 626.1[a]
Cerebrum	0.8 ± 0.2	34.3 ± 4.2[a]	110.9 ± 41.0[a]
Heart	1.4 ± 0.2	27.6 ± 5.6[a]	30.2 ± 9.3[a]
Kidney	1.9 ± 0.1	43.5 ± 5.9[a]	68.3 ± 10.5[a]
Acylated ghrelin			
Plasma (fmol/ml)	83.7 ± 11.9	79.7 ± 10.6	86.3 ± 21.1
Tissues (fmol/mg)			
Stomach	413.0 ± 46.7	341.2 ± 66.8	325.0 ± 49.5
Cerebrum	0.05>	0.05>	0.05>
Heart	0.1 ± 0.0	0.05>	0.05>
Kidney	0.1 ± 0.0	0.1 ± 0.1	0.1 ± 0.0

Values are given as the mean ± SEM.
[a] $P < 0.01$ *vs.* control mice.

transgenic mice are shown in Table 3. Eight-week-old male Tg 9–2 and Tg 10–1 mice were significantly shorter in the body length than control mice ($P < 0.05$ and $P < 0.01$, respectively). Female Tg 10–1 mice were significantly shorter than control mice ($P < 0.01$). The difference between female control and Tg 9–2 mice was not significant. BMIs were calculated from the body weights and lengths. No significant difference was noted between control and Tg 9–2 mice and control and Tg 10–1 mice (Table 3). Fifty-two-week-old male Tg 9–2 and Tg10–1 mice were still significantly lighter and shorter, compared with control mice (Table 3), and no significant difference was noted in BMIs between control and transgenic mice. Relative organ weights of 8-wk-old male control and Tg 10–1 mice were calculated from the organ and body weights. No significant difference was noted between control and Tg 10–1 mice (Fig. 2B). No significant difference was noted in the pituitary size between control and Tg 10–1 mice (0.058 ± 0.002 and 0.055 ± 0.003 mg/body weight (grams), respectively).

TABLE 3. Body weights, lengths, and BMIs of 8-wk-old and 52-wk-old control and transgenic mice (n = 8/group)

		Control	Tg 9-2	Tg 10-1
Male				
8-wk-old	Body weight (g)	23.2 ± 0.5	21.0 ± 0.7[a]	16.6 ± 0.6[b]
	Nose-to-anus length (cm)	9.2 ± 0.3	8.6 ± 0.1[a]	7.7 ± 0.3[b]
	BMI (g/cm^2)	27.1 ± 1.2	28.1 ± 3.1[c]	27.3 ± 1.9[c]
52-wk-old	Body weight (g)	34.7 ± 0.8	31.2 ± 0.6[a]	28.4 ± 0.1[b]
	Nose-to-anus length (cm)	10.1 ± 0.1	9.5 ± 0.3[a]	9.1 ± 0.1[b]
	BMI (g/cm^2)	34.4 ± 0.8	34.7 ± 0.6[c]	34.5 ± 0.8[c]
Female				
8-wk-old	Body weight (g)	16.6 ± 1.2	18.7 ± 0.7[c]	10.7 ± 1.1[b]
	Nose-to-anus length (cm)	8.1 ± 0.6	8.5 ± 0.2[c]	6.4 ± 0.2[b]
	BMI (g/cm^2)	25.8 ± 1.8	26.2 ± 1.2[c]	26.5 ± 1.5[c]
52-wk-old	Body weight (g)	25.3 ± 1.3	24.8 ± 0.8[c]	19.6 ± 0.7[b]
	Nose-to-anus length (cm)	9.0 ± 0.4	8.9 ± 0.3[c]	7.9 ± 0.2[b]
	BMI (g/cm^2)	30.9 ± 1.0	31.2 ± 0.7[c]	31.3 ± 1.1[c]

Values are given as the mean ± SEM.
[a] $P < 0.05$ *vs.* control mice.
[b] $P < 0.01$ *vs.* control mice.
[c] Not significant.

Immunohistochemical staining for total and acylated ghrelin of the pituitary

Immunohistochemical staining for total and acylated ghrelin is shown in Fig. 3, A–D. None of total ghrelin-positive cells were observed in the pituitary of control mice (Fig. 3A). On the other hand, many total ghrelin-immunoreactive pituitary cells were observed in Tg 10–1 mice (Fig. 3B). Approximately 30% of the anterior pituitary cells in all sections examined were total ghrelin immunoreactive. None of acylated ghrelin-positive cells were observed in the pituitary of either control or Tg 10–1 mice (Fig. 3, C and D).

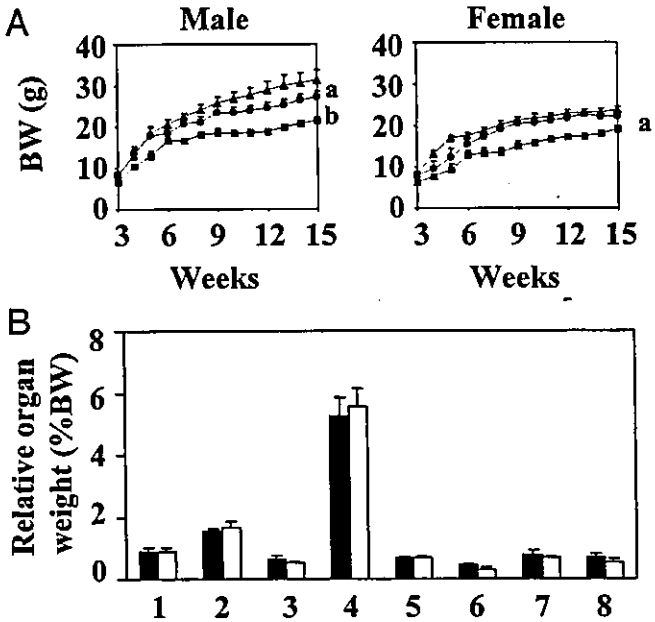

FIG. 2. Body weights (BW) and relative organ weights. A, Body weights of male (*left panel*) and female (*right panel*) control (*triangles*), Tg 9–2 (*circles*), and Tg 10–1 (*squares*) mice (n = 8/group). B, Relative organ weights of 8-wk-old control (*closed bars*) and Tg 10–1 (*open bars*) mice calculated from the organ and body weights (n = 8/group). 1, stomach; 2, cerebrum; 3, heart; 4, liver; 5, kidney; 6, spleen; 7, pancreas; 8, epididymal fat. a, $P < 0.05$; b, $P < 0.01$ (*vs.* control mice).

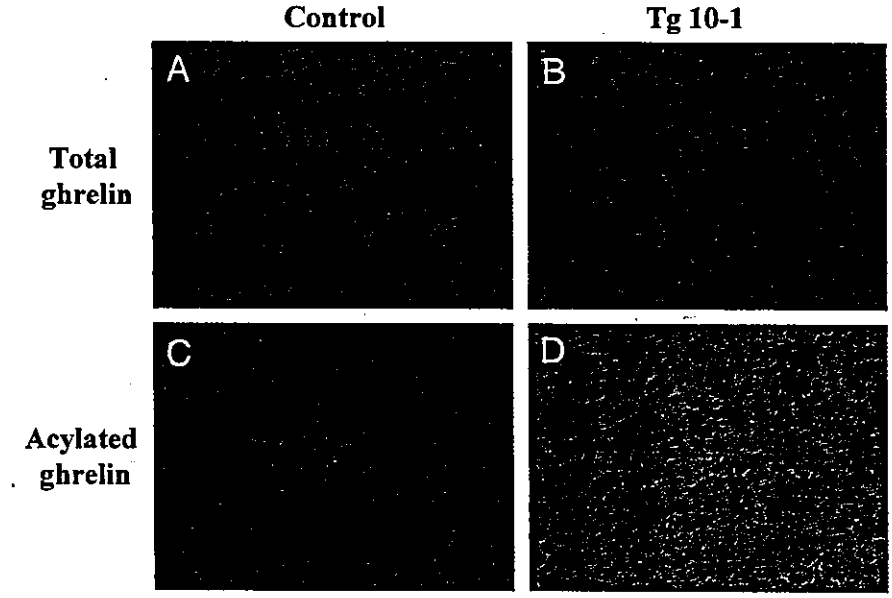

FIG. 3. The localization of total and acylated ghrelin-immunoreactive cells in the pituitary of 8-wk-old male control (A and C) and Tg 10–1 (B and D) mice. A and B, An antiserum raised to ghrelin(13–28) recognizing total (acylated plus des-acyl) ghrelin was used. C and D, An antiserum raised to ghrelin(1–11) specifically recognizing acylated ghrelin was used. Original magnification, ×40. The immunoreactive cells are stained *brown* by the avidin-biotin complex methods.

Food intake and biochemical parameters in the blood

Although absolute amounts of daily food intake were reduced in Tg 9–2 and Tg 10–1 mice, the amounts per body weight were not significantly changed in either male or female Tg 9–2 or Tg 10–1 mice, compared with control mice (Table 4). No significant differences in blood glucose, serum total protein, total cholesterol, and insulin levels were noted between 8-wk-old control and Tg 9–2 mice and control and Tg 10–1 mice (Table 4).

Serum GH, IGF-1, and pituitary GH mRNA levels

Serum GH levels in male control, Tg 9–2, and Tg 10–1 mice were 5.5 ± 1.9, 3.7 ± 0.7, and 2.3 ± 0.9 ng/ml, respectively (Fig. 4A). Those in female control, Tg 9–2, and Tg 10–1 mice were 4.7 ± 1.7, 2.5 ± 0.9, and 1.7 ± 0.8 ng/ml, respectively (Fig. 4A). There were tendencies for decline in serum GH levels in male and female Tg 9–2 and Tg 10–1 mice, compared with control mice, although the differences between them were not significant. Serum IGF-I levels in male control, Tg 9–2, and Tg 10–1 mice were 522 ± 23.6, 413.2 ± 49.0, and 364.1 ± 25.6 ng/ml, respectively (Fig. 4B). Those in male Tg 9–2 and Tg 10–1 mice were significantly reduced, compared with those in control mice ($P < 0.01$ for each). Serum IGF-I levels in female control, Tg 9–2, and Tg 10–1 mice were 509.7 ± 43.1, 545.5 ± 64.1, and 253.7 ± 36.4 ng/ml, respectively (Fig. 4B). Those in female Tg 10–1 mice were significantly reduced, compared with those in control mice ($P < 0.01$). The difference between female control and Tg 9–2 mice was not significant.

Pituitary GH mRNA levels in male control, Tg 9–2, and Tg 10–1 mice were 1.00, 0.62, and 0.42 AU, respectively. Those in Tg 9–2 and Tg 10–1 mice were significantly reduced, compared with those in control mice ($P < 0.05$ and $P < 0.01$, respectively). Pituitary GH mRNA levels in female control, Tg 9–2, and Tg 10–1 mice were 1.00, 0.97, and 0.71 AU. Those in female Tg 10–1 mice were significantly reduced, compared with those in control mice ($P < 0.05$). The difference between those in female control and Tg 9–2 mice was not significant (Fig. 4C).

Plasma ACTH, serum TSH, LH, and FSH levels

Plasma ACTH, serum TSH, LH, and FSH levels in 8-wk-old in male control and transgenic mice are shown in Table

TABLE 4. Daily food intake, blood glucose, serum total protein, total cholesterol, and insulin levels in 8-wk-old control and transgenic mice (n = 8/group)

	Control	Tg 9-2	Tg 10-1
Male			
Daily food intake (mg/BW/d)	149.1 ± 7.6	154.2 ± 3.2	155.2 ± 5.9
Serum total protein (mg/dl)	5.1 ± 0.2	4.9 ± 0.1	5.5 ± 0.1
Serum total cholesterol (mg/dl)	121.0 ± 12	116.9 ± 11.3	123.1 ± 8.3
Blood sugar (mg/dl)	134.2 ± 9.4	135.3 ± 8.7	136.7 ± 5.8
Serum insulin (pg/ml)	3233 ± 407	4624 ± 1015	2419 ± 423
Female			
Daily food intake (mg/BW/d)	167.5 ± 2.3	169.5 ± 4.7	165.8 ± 9.8
Serum total protein (mg/dl)	5.4 ± 0.1	5.1 ± 0.3	5.2 ± 0.3
Serum total cholesterol (mg/dl)	129.0 ± 9.3	123.4 ± 9.2	122.9 ± 6.1
Blood sugar (mg/dl)	132.1 ± 5.5	134.2 ± 6.4	130.6 ± 7.2
Serum insulin (pg/ml)	1182 ± 284	2079 ± 587	1799 ± 725

Values are given as the mean ± SEM. BW, Body weight.

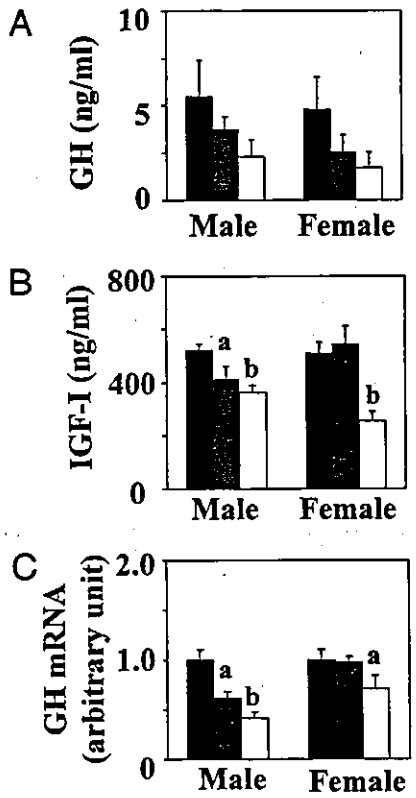

FIG. 4. Serum GH, IGF-I, and pituitary GH mRNA levels in 8-wk-old control (*closed bars*), Tg 9–2 (*shaded bars*), and Tg 10–1 (*open bars*) mice (n = 8/group). A, Serum GH levels. B, Serum IGF-I levels. C, Pituitary GH mRNA levels. a, $P < 0.05$; b, $P < 0.01$ (*vs.* control mice).

5. No significant difference was noted in the levels between control and transgenic mice.

Hematoxylin eosin and immunohistochemical staining for GH of the pituitary

Hematoxylin eosin staining is shown in Fig. 5, A and B. The pituitary morphology of Tg 10–1 mice was not different from that of the control mice. Immunohistochemical staining for GH is shown in Fig. 5, C and D. The distribution of GH-immunoreactive cells in the pituitary of Tg mice was similar to that of control mice.

Effects of GHRH and ghrelin on GH release

Control and Tg 10–1 mice were used. Serum GH levels after GHRH administration in male and female Tg 10–1 mice were similar to those of control mice throughout the course of the experiment (Fig. 6A). There was no significant difference in serum GH level at each time point between both male and female Tg-10 and control mice. Serum GH levels 10 min after ghrelin administration in male Tg10–1 and control mice were 63.1 ± 6.8 and 72.6 ± 12.0 ng/ml, respectively (Fig. 6B, *left panel*). The difference was not significant. Serum GH levels 20 min after ghrelin administration in male Tg10–1 and control mice were 30.2 ± 6.7 and 61.2 ± 15.5 ng/ml, respectively, and levels after 30 min were 11.8 ± 1.4 and 21.9 ± 4.1 ng/ml, respectively (Fig. 6B, *left panel*). Both differences were significant ($P < 0.01$). Serum GH levels 10 min after ghrelin administration in female Tg10–1 and control mice were 8.7 ± 3.7 and 52.8 ± 8.2 ng/ml, respectively, and those after 20 min were 29.8 ± 6.3 and 78.5 ± 14.3 ng/ml, respectively (Fig. 6B, *right panel*). Both differences were significant ($P < 0.01$). Serum GH levels 30 min after ghrelin administration in female Tg10–1 and control mice were 22.8 ± 6.3 and 22.3 ± 8.8 ng/ml, respectively (Fig. 6B, *right panel*). The difference was not significant.

TABLE 5. Plasma ACTH, serum TSH, LH, and FSH levels of 8-wk-old control and transgenic mice (n = 8/group)

	Control	Tg 9-2	Tg 10-1
ACTH (pg/ml)	135 ± 35	144 ± 32	123 ± 44
TSH (ng/ml)	3.31 ± 0.06	3.37 ± 0.11	3.49 ± 0.13
LH (ng/ml)	31.5 ± 2.1	30.8 ± 1.7	27.7 ± 2.1
FSH (ng/ml)	268.4 ± 21.8	221.1 ± 43.9	253.5 ± 24.6

Values are given as the mean ± SEM.

Expression of GHS-R in the pituitary

GHS-R mRNA levels of male control, Tg 9–2, and Tg 10–1 mice were 1.00, 1.56, and 3.46 AU, respectively (Fig. 7). The difference between control and Tg 10–1 mice was significant ($P < 0.01$).

Expression of hypothalamic neuropeptides that regulate GH secretion

GHRH mRNA levels of male control, Tg 9–2, and Tg 10–1 mice were 1.00, 0.88, and, 0.80 AU, respectively (Fig. 8A). The differences between control and Tg 9–2 mice and control and Tg 10–1 mice were not significant. Somatostatin mRNA levels of male control, Tg 9–2, and Tg 10–1 mice were 1.00, 1.08, and 0.97 AU, respectively (Fig. 8B). The differences between control and Tg 9–2 mice and control and Tg 10–1 mice were not significant.

Effects of continuous infusion of des-acyl ghrelin on GH-IGF-I axis and body weights

Male and female C57BL/6 mice were used. Serum GH levels after 10 d treatment with saline and des-acyl ghrelin in male mice were 5.8 ± 1.1 and 7.5 ± 2.0 ng/ml, respectively. The difference was not significant. Those with saline and des-acyl ghrelin in female mice were 9.2 ± 2.2 and 9.5 ± 1.8 ng/ml, respectively. The difference was not significant either. Serum IGF-I levels after 10 d treatment with saline and des-acyl ghrelin in male mice were 769.3 ± 16.6 and 768.7 ± 21.6 ng/ml, respectively. The difference was not significant. Those with saline and des-acyl ghrelin in female mice were 766.2 ± 13.4 and 719.4 ± 49.1 ng/ml, respectively. The difference was not significant either. Body weights and lengths in des-acyl ghrelin-injected mice were not significantly different from those in saline-injected mice in either males or females (data not shown).

Discussion

We have generated transgenic mouse lines that overexpress preproghrelin mRNA in a wide variety of tissues. The wide tissue distribution of preproghrelin mRNA in trans-

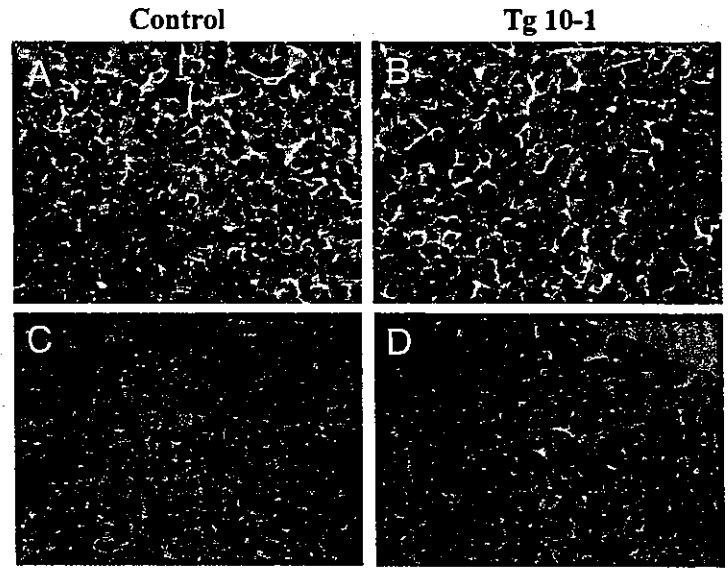

FIG. 5. Morphology of the pituitary and the localization of GH-immunoreactive cells in the pituitary of 8-wk-old male control (A and C) and Tg 10–1 (B and D) mice. A and B, Hematoxylin eosin (HE) staining. C and D, The localization of total and GH-immunoreactive cells in the pituitary. Original magnification, ×40. The immunoreactive cells are stained *brown* by the avidin-biotin complex methods.

genic mice was consistent with previous reports on transgenic mice using the CAG promoter (33, 34). Preproghrelin mRNA expression was increased, especially in Tg 10–1 mice, and its amount in the stomach reached 52-fold of that in control mice. Consistent with the elevated mRNA expression, peptide levels of total ghrelin (des-acyl plus acylated ghrelin) in various tissues were also elevated in transgenic mice. Plasma total ghrelin levels in transgenic mice showed marked results. Those in transgenic mice showed 10- and 44-fold of those in control mice. We originally intended to generate mice overexpressing biologically active ghrelin. Unexpectedly, acylated ghrelin levels were not changed in all tissues examined and plasma of transgenic mice, compared with those of control mice, indicating that transgenic mice overexpress only des-acyl ghrelin. The expression of acylated ghrelin has been reported in a small number of tissues, such as the stomach (X/A cells), duodenum, hypothalamus, and pancreatic α-cells (1, 31, 39, 40). These reports and our present data suggest that only a limited number of cell lineages may able to process proghrelin or acylate ghrelin. The underlying mechanism by which ghrelin is acylated is unknown to date. Further study is needed to clarify the mechanism of the acylation.

The acylation of ghrelin is assumed to be essential for its actions, and des-acyl ghrelin, which lacks the modification, is devoid of endocrine actions, based on previous studies (1, 41). However, recent studies indicated that des-acyl ghrelin may have some actions. Des-acyl ghrelin as well as acylated ghrelin causes a significant inhibition of cell proliferation in human breast carcinoma cell lines (29) and inhibits cell death in cardiomyocytes and endothelial cells through ERK1/2 and phosphatidylinositol 3-kinase/AKT (30). In addition, one study (42) reported that acylated and des-acyl ghrelin promote adipogenesis directly *in vivo* by a mechanism independent of known GHS-Rs. Moreover, another study (28) indicated that des-acyl ghrelin may offset the action of acylated ghrelin on insulin secretion. Ghrelin has been shown to induce a reduction in serum insulin levels. In the study, coadministration of acylated plus des-acyl ghrelin did not re-

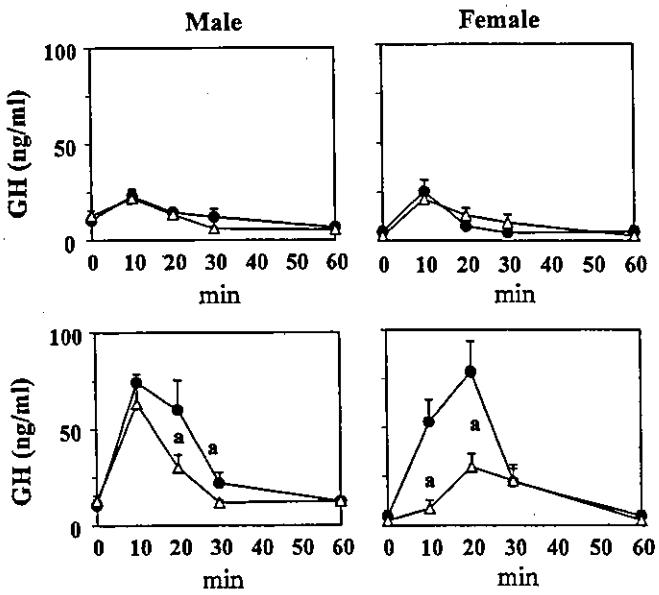

FIG. 6. The responses of GH to GHRH and ghrelin in 8-wk-old control (*closed circles*) and Tg 10–1 (*open triangles*) mice. A, Time course of serum GH levels after iv injection of 60 μg/kg GHRH (n = 8/each point). B, Time course of serum GH levels after iv injection of 40 μg/kg ghrelin (n = 8/each point). a, $P < 0.01$ (*vs.* control mice).

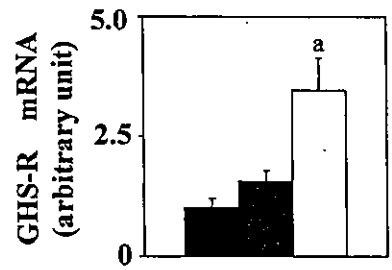

FIG. 7. Pituitary GHS-R mRNA levels in 8-wk-old control (*closed bars*), Tg 9–2 (*shaded bars*), and Tg 10–1 (*open bars*) mice quantified by real-time PCR analysis (n = 8/group). a, $P < 0.01$ (*vs.* control mice).

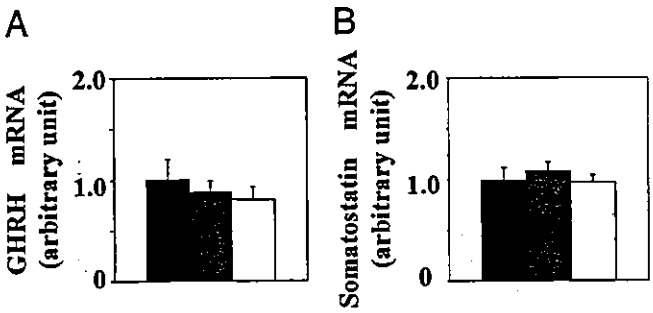

FIG. 8. Hypothalamic GHRH and somatostatin mRNA levels in 8-wk-old control (*closed bars*), Tg 9–2 (*shaded bars*), and Tg 10–1 (*open bars*) mice quantified by real-time PCR analysis. A, GHRH mRNA levels (n = 8/group). B, Somatostatin mRNA levels (n = 8/group).

sult in any changes in serum insulin levels in humans, suggesting that ghrelin action on insulin is modulated by des-acyl ghrelin.

The present study indicates that transgenic mice overexpressing des-acyl ghrelin show small phenotype. Longitudinal growth was the most reduced in female Tg 10–1 mice (20% reduction from control mice). The phenotype was not associated with changes in BMIs. These mice did not show decreased food intake or decreased body fat mass. In addition, they showed normal nutritional condition, based on their biochemical parameters, including blood glucose, serum total protein, and total cholesterol levels. These data indicate that the small phenotype of transgenic mice is not attributed to poor nutritional condition.

Serum IGF-I levels were significantly reduced in male and female transgenic mice, compared with control mice. Female Tg 10–1 mice had no less than 50% reduction in serum IGF-I levels, compared with control mice. Although the differences in serum GH levels between control and transgenic mice were not statistically significant, probably because of the pulsatile character of GH secretion, the levels tended to be reduced in transgenic mice, compared with control mice, and the mean GH level of Tg10–1 mice was only 50% of that of control mice. It should be emphasized that Tg 10–1 mice showed lower serum GH levels than Tg 9–2 mice. Body weights and lengths of the former were more reduced than the latter. It should be also noted that the former showed higher des-acyl ghrelin expression than the latter. Reduced pituitary GH mRNA levels in transgenic mice support the observation. The GH-IGF-I axis-specific alteration in transgenic mice was also indicated by the measurement of other anterior pituitary hormones than GH. Plasma ACTH, serum TSH, LH, and FSH levels were not altered.

The size and morphology of the pituitary including the somatotrope populations of transgenic mice were similar to those of control mice. These data indicated that there is no apparent change, suggesting developmental problems in the pituitary of transgenic mice.

Responses of GH to GHRH and ghrelin in transgenic mice exhibited intriguing results. Transgenic mice showed normal response of GH to GHRH. Alternatively, if we consider that the basal GH levels are lower in transgenic mice, the similar maximal response might indicate that they are hyperresponsive to GHRH. It is not likely that an insufficient dose of GHRH induced submaximal response of GH in both control and transgenic mice, judging from previous reports (43). On the other hand, the responses of GH to ghrelin were reduced in transgenic mice. It is noteworthy that the reduction was much greater in female transgenic mice than in male mice, if we take their serum IGF-I levels into account. Taken together our results and these reports indicate that overexpression of des-acyl ghrelin in our mice may result in reduction of GH response to endogenous ghrelin, and it may result in the reduced serum IGF-I levels in transgenic mice.

The reduced GH response to ghrelin in transgenic mice could be due to down-regulated the GHS-R. However, the pituitary GHS-R mRNA levels in the transgenic mice were rather elevated. It is not likely that overexpressed des-acyl ghrelin acts as a blocking agent to the GHS-R because ^{125}I-labeled acylated ghrelin bound to the GHS-R cannot be displaced by des-acyl ghrelin (20). Overexpressed des-acyl ghrelin may have some effects on endogenous GH secretion, modifying the action of endogenous ghrelin in transgenic mice via, for instance, another receptor or modulation of the signal transduction pathway after the GHS-R.

Previous reports indicated that the hypothalamus plays a critical role in the stimulatory effect of ghrelin on GH secretion as well as the pituitary (21, 22, 23). Because GH secretion is regulated chiefly by two hypothalamic hormones, GHRH and somatostatin, the expression of these hormones could be altered in transgenic mice. We could not find any significant difference in either GHRH or somatostatin mRNA levels between control and transgenic mice. These data might suggest that overexpressed des-acyl ghrelin acts on not only the pituitary but also the hypothalamus in the transgenic mice, judging from the fact that hypothalamus GHRH mRNA were not elevated, and somatostatin mRNA levels were not decreased despite the decreased serum GH levels.

We could not show, unfortunately, that continuous ip infusion of des-acyl ghrelin has some effect on serum GH and IGF-I levels or body weights. It should be noted, however, that plasma des-acyl ghrelin levels in transgenic mice reached 10- and 50-fold of those in control mice. Administration of a higher dose of des-acyl ghrelin, or longer administration, might result in alteration in the GH-IGF-I axis. On the other hand, the phenotype of transgenic mice might reflect direct effects of ubiquitous expression of des-acyl ghrelin. It should also be noted that high levels of des-acyl ghrelin were detected in a various tissues, especially in the pituitary, as well as in plasma of transgenic mice. The des-acyl ghrelin immunoreactive pituitary cells might play an important role in the mechanism for the altered GH-IGF-I axis in a paracrine or autocrine manner. It should be pointed out that preproghrelin mRNA is reported to be expressed in the normal pituitary (44), as we showed in the present study, suggesting its physiological role in GH secretion. The phenotype of transgenic mice may reflect the role. Further study is needed for this issue.

The mechanism underlying the sexual dimorphism in the responses of GH to ghrelin in transgenic mice is not fully understood. It might be due to the gender difference in the secretory regulation of GH. Female mice have been reported to be different from male mice in that they have noncyclical

and rather low somatostatin output and that GHRH plays a dominant role in it (45). There might be a GHRH-dependent mechanism for the reduced response in transgenic mice. Indeed, one recent report (26) indicated that transgenic rats expressing an antisense GHS-R mRNA in the hypothalamic arcuate nucleus show marked gender difference in GH secretion. Although there was no significant difference in pulse frequency and baseline levels of GH between male control and transgenic rats, female transgenic rats showed lower baseline levels and fewer pulses of GH than female control rats (26).

The 94-amino acid proghrelin is cleaved to yield ghrelin. One previous study (46) demonstrated that C-terminal proghrelin peptides are present in the human circulation. Transgenic mice in the present study would also overexpress these peptides. We have not excluded the possibility that the phenotype of transgenic mice might be due to the effects of these peptides.

In conclusion, the present study demonstrates that transgenic mice overexpressing des-acyl ghrelin show small phenotype and altered GH-IGF-I axis. These observations may indicate a role of des-acyl ghrelin in the regulation of GH secretion.

Acknowledgments

The authors gratefully acknowledge the excellent technical support of Chieko Ishimoto and Hitomi Hiratani.

Received May 17, 2004. Accepted October 1, 2004.

Address all correspondence and requests for reprints to: Kazuhiko Takaya, M.D., Ph.D., Translational Research Center, Kyoto University Hospital, Kyoto 606-8507, Japan. E-mail: ktakaya@kuhp.kyoto-u.ac.jp.

This work was supported by research grants from the Japanese Ministry of Education, Science, and Culture and the Japanese Ministry of Health, Labor, and Welfare.

References

1. Kojima M, Hosoda H, Date Y, Nakazato M, Matsuo H, Kangawa K 1999 Ghrelin is a growth-hormone-releasing acylated peptide from stomach. Nature 402:656–660
2. Date Y, Murakami N, Kojima M, Kuroiwa T, Matsukura S, Kangawa K, Nakazato M 2000 Central effects of a novel acylated peptide, ghrelin, on growth hormone release in rats. Biochem Biophys Res Commun 275:477–480
3. Ariyasu H, Takaya K, Tagami T, Ogawa Y, Hosoda K, Akamizu T, Suda M, Koh T, Natsui K, Toyooka S, Shirakami G, Usui T, Shimatsu A, Doi K, Hosoda H, Kojima M, Kangawa K, Nakao K 2001 Stomach is a major source of circulating ghrelin, and feeding state determines plasma ghrelin-like immunoreactivity levels in humans. J Clin Endocrinol Metab 86:4753–4758
4. Lu S, Guan JL, Wang QP, Uehara K, Yamada S, Goto N, Date Y, Nakazato M, Kojima M, Kangawa K, Shioda S 2001 Immunocytochemical observation of ghrelin-containing neurons in the rat arcuate nucleus. Neurosci Lett 321: 157–160
5. Cowley MA, Smith RG, Diano S, Tschop M, Pronchuk N, Grove KL, Strasburger CJ, Bidlingmaier M, Esterman M, Heiman ML, Garcia-Segura LM, Nillni EA, Mendez P, Low MJ, Sotonyi P, Friedman JM, Liu H, Pinto S, Colmers WF, Cone RD, Horvath TL 2003 The distribution and mechanism of action of ghrelin in the CNS demonstrates a novel hypothalamic circuit regulating energy homeostasis. Neuron 37:649–661
6. Cummings DE, Purnell JQ, Frayo RS, Schmidova K, Wisse BE, Weigle DS 2001 A preprandial rise in plasma ghrelin levels suggests a role in meal initiation in humans. Diabetes 50:1714–1719
7. Asakawa A, Inui A, Kaga T, Yuzuriha H, Nagata T, Ueno N, Makino S, Fujimiya M, Niijima A, Fujino MA, Kasuga M 2001 Ghrelin is an appetite-stimulatory signal from stomach with structural resemblance to motilin. Gastroenterology 120:337–345
8. Nakazato M, Murakami N, Date Y, Kojima M, Matsuo H, Kangawa K, Matsukura S 2001 A role for ghrelin in the central regulation of feeding. Nature 409:194–198
9. Ariyasu H, Takaya K, Hosoda H, Iwakura H, Ebihara K, Mori K, Ogawa Y, Hosoda K, Akamizu T, Kojima M, Kangawa K, Nakao K 2002 Delayed short-term secretory regulation of ghrelin in obese animals: evidenced by a specific RIA for the active form of ghrelin. Endocrinology 143:3341–3350
10. Tschop M, Weyer C, Tataranni PA, Devanarayan V, Ravussin E, Heiman ML 2001 Circulating ghrelin levels are decreased in human obesity. Diabetes 50: 707–709
11. Hanada T, Toshinai K, Kajimura N, Nara-Ashizawa N, Tsukada T, Hayashi Y, Osuye K, Kangawa K, Matsukura S, Nakazato M 2003 Anti-cachectic effect of ghrelin in nude mice bearing human melanoma cells. Biochem Biophys Res Commun 301:275–279
12. Shintani M, Ogawa Y, Ebihara K, Aizawa-Abe M, Miyanaga F, Takaya K, Hayashi T, Inoue G, Hosoda K, Kojima M, Kangawa K, Nakao K 2001 Ghrelin, an endogenous growth hormone secretagogue, is a novel orexigenic peptide that antagonizes leptin action through the activation of hypothalamic neuropeptide Y/Y1 receptor pathway. Diabetes 50:227–232
13. Wren AM, Small CJ, Abbott CR, Dhillo WS, Seal IJ, Cohen MA, Batterham RL, Taheri S, Stanley SA, Ghatei MA, Bloom SR 2001 Ghrelin causes hyperphagia and obesity in rats. Diabetes 50:2540–2547
14. Dieguez C, Casanueva FF 2000 Ghrelin: a step forward in the understanding of somatotroph cell function and growth regulation. Eur J Endocrinol 142: 413–417
15. Seoane LM, Tovar S, Baldelli R, Arvat E, Ghigo E, Casanueva FF, Dieguez C 2000 Ghrelin elicits a marked stimulatory effect on GH secretion in freely moving rats. Eur J Endocrinol 143:R7–R9
16. Takaya K, Ariyasu H, Kanamoto N, Iwakura H, Yoshimoto A, Harada M, Mori K, Komatsu Y, Usui T, Shimatsu A, Ogawa Y, Hosoda K, Akamizu T, Kojima M, Kangawa K, Nakao K 2000 Ghrelin strongly stimulates growth hormone release in humans. J Clin Endocrinol Metab 85:4908–4911
17. Guan XM, Yu H, Palyha OC, McKee KK, Feighner SD, Sirinathsinghji DJ, Smith RG, Van der Ploeg LH, Howard AD 1997 Distribution of mRNA encoding the growth hormone secretagogue receptor in brain and peripheral tissues. Brain Res Mol Brain Res 48:23–29
18. Gnanapavan S, Kola B, Bustin SA, Morris DG, McGee P, Fairclough P, Bhattacharya S, Carpenter R, Grossman AB, Korbonits M 2002 The tissue distribution of the mRNA of ghrelin and subtypes of its receptor, GHS-R, in humans. J Clin Endocrinol Metab 87:2988
19. Willesen MG, Kristensen P, Romer J 1999 Co-localization of growth hormone secretagogue receptor and NPY mRNA in the arcuate nucleus of the rat. Neuroendocrinology 70:306–316
20. Muccioli G, Papotti M, Locatelli V, Ghigo E, Deghenghi R 2001 Binding of ^{125}I-labeled ghrelin to membranes from human hypothalamus and pituitary gland. J Endocrinol Invest 24:RC7–RC9
21. Torsello A, Grilli R, Luoni M, Guidi M, Ghigo MC, Wehrenberg WB, Deghenghi R, Muller EE, Locatelli V 1996 Mechanism of action of hexarelin. I. Growth hormone-releasing activity in the rat. Eur J Endocrinol 135:481–488
22. Maheshwari HG, Rahim A, Shalet SM, Baumann G 1999 Selective lack of growth hormone (GH) response to the GH-releasing peptide hexarelin in patients with GH-releasing hormone receptor deficiency. J Clin Endocrinol Metab 84:956–959
23. Hataya Y, Akamizu T, Takaya K, Kanamoto N, Ariyasu H, Saijo M, Moriyama K, Shimatsu A, Kojima M, Kangawa K, Nakao K 2001 A low dose of ghrelin stimulates growth hormone (GH) release synergistically with GH-releasing hormone in humans. J Clin Endocrinol Metab 86:4552–4555
24. Okimura Y, Ukai K, Hosoda H, Murata M, Iguchi G, Iida K, Kaji H, Kojima M, Kangawa K, Chihara K 2003 The role of circulating ghrelin in growth hormone (GH) secretion in freely moving male rats. Life Sci 72:2517–2524
25. Sun Y, Ahmed S, Smith RG 2003 Deletion of ghrelin impairs neither growth nor appetite. Mol Cell Biol 23:7973–7981
26. Shuto Y, Shibasaki T, Otagiri A, Kuriyama H, Ohata H, Tamura H, Kamegai J, Sugihara H, Oikawa S, Wakabayashi I 2002 Hypothalamic growth hormone secretagogue receptor regulates growth hormone secretion, feeding, and adiposity. J Clin Invest 109:1429–1436
27. Hosoda H, Kojima M, Matsuo H, Kangawa K 2000 Ghrelin and des-acyl ghrelin: two major forms of rat ghrelin peptide in gastrointestinal tissue. Biochem Biophys Res Commun 279:909–913
28. Broglio F, Prodam F, Benso A, Gottero C, Destefanis S, Gauna C, van der Lely AJ, Ghigo E, The peripheral but not the neuro-endocrine response to acylated ghrelin is modulated by non-acylated ghrelin in humans. Program of the 85th Annual Meeting of The Endocrine Society, Philadelphia, PA, 2003, p 264 (Abstract P1-553)
29. Cassoni P, Papotti M, Ghe C, Catapano F, Sapino A, Graziani A, Deghenghi R, Reissmann T, Ghigo E, Muccioli G 2001 Identification, characterization, and biological activity of specific receptors for natural (ghrelin) and synthetic growth hormone secretagogues and analogs in human breast carcinomas and cell lines. J Clin Endocrinol Metab 86:1738–1745
30. Baldanzi G, Filigheddu N, Cutrupi S, Catapano F, Bonissoni S, Fubini A, Malan D, Baj G, Granata R, Broglio F, Papotti M, Surico N, Bussolino F, Isgaard J, Deghenghi R, Sinigaglia F, Prat M, Muccioli G, Ghigo E, Graziani A 2002 Ghrelin and des-acyl ghrelin inhibit cell death in cardiomyocytes and endothelial cells through ERK1/2 and PI 3-kinase/AKT. J Cell Biol 159:1029–1037
31. Iwakura H, Hosoda K, Doi R, Komoto I, Nishimura H, Son C, Fujikura J,

Tomita T, Takaya K, Ogawa Y, Hayashi T, Inoue G, Akamizu T, Hosoda H, Kojima M, Kangawa K, Imamura M, Nakao K 2002 Ghrelin expression in islet cell tumors: augmented expression of ghrelin in a case of glucagonoma with multiple endocrine neoplasm type I. J Clin Endocrinol Metab 87:4885–4888
32. Mori K, Yoshimoto A, Takaya K, Hosoda K, Ariyasu H, Yahata K, Mukoyama M, Sugawara A, Hosoda H, Kojima M, Kangawa K, Nakao K 2000 Kidney produces a novel acylated peptide, ghrelin. FEBS Lett 486:213–216
33. Ikawa M, Kominami K, Yoshimura Y, Tanaka K, Nishimune Y, Okabe M 1995 Green fluorescent protein as a marker in transgenic mice. Dev Growth Differ 37:455–459
34. Niwa H, Yamamura K, Miyazaki J 1991 Efficient selection for high-expression transfectants with a novel eukaryotic vector. Gene 108:193–199
35. Ogawa Y, Masuzaki H, Hosoda K, Aizawa-Abe M, Suga J, Suda M, Ebihara K, Iwai H, Matsuoka N, Satoh N, Odaka H, Kasuga H, Fujisawa Y, Inoue G, Nishimura H, Yoshimasa Y, Nakao K 1999 Increased glucose metabolism and insulin sensitivity in transgenic skinny mice overexpressing leptin. Diabetes 48:1822–1829
36. Bahary N, Leibel RL, Joseph L, Friedman JM 1990 Molecular mapping of the mouse db mutation. Proc Natl Acad Sci USA 87:8642–8646
37. Maffei M, Halaas J, Ravussin E, Pratley RE, Lee GH, Zhang Y, Fei H, Kim S, Lallone R, Ranganathan S 1995 Leptin levels in human and rodent: measurement of plasma leptin and ob RNA in obese and weight-reduced subjects. Nat Med 1:1155–1161
38. Chomczynski P, Sacchi N 1987 Single-step method of RNA isolation by acid guanidinium thiocyanate-phenol-chloroform extraction. Anal Biochem 162: 156–159
39. Date Y, Kojima M, Hosoda H, Sawaguchi A, Mondal MS, Suganuma T, Matsukura S, Kangawa K, Nakazato M 2000 Ghrelin, a novel growth hormone-releasing acylated peptide, is synthesized in a distinct endocrine cell type in the gastrointestinal tracts of rats and humans. Endocrinology 141: 4255–4261
40. Date Y, Nakazato M, Hashiguchi S, Dezaki K, Mondal MS, Hosoda H, Kojima M, Kangawa K, Arima T, Matsuo H, Yada T, Matsukura S 2002 Ghrelin is present in pancreatic α-cells of humans and rats and stimulates insulin secretion. Diabetes 51:124–129
41. Broglio F, Benso A, Gottero C, Prodam F, Gauna C, Filtri L, Arvat E, van der Lely AJ, Deghenghi R, Ghigo E 2003 Non-acylated ghrelin does not possess the pituitaric and pancreatic endocrine activity of acylated ghrelin in humans. J Endocrinol Invest 26:192–196
42. Thompson NM, Gill DA, Davies R, Loveridge N, Houston PA, Robinson IC, Wells T 2004 Ghrelin and des-octanoyl ghrelin promote adipogenesis directly *in vivo* by a mechanism independent of the type 1a growth hormone secretagogue receptor. Endocrinology 145:234–242
43. Clark RG, Robinson IC 1985 Effects of a fragment of human growth hormone-releasing factor in normal and 'little' mice. J Endocrinol 106:1–5
44. Kamegai J, Tamura H, Shimizu T, Ishii S, Sugihara H, Oikawa S 2001 Regulation of the ghrelin gene: growth hormone-releasing hormone upregulates ghrelin mRNA in the pituitary. Endocrinology 142:4154–4157
45. Robinson IC 1991 The growth hormone secretory pattern: a response to neuroendocrine signals. Acta Paediatr Scand Suppl 372:70–78;discussion 79–80
46. Pemberton C, Wimalasena P, Yandle T, Soule S, Richards M 2003 C-terminal pro-ghrelin peptides are present in the human circulation. Biochem Biophys Res Commun 310:567–573

Endocrinology **is published monthly by The Endocrine Society (http://www.endo-society.org), the foremost professional society serving the endocrine community.**

Overexpression of Brain Natriuretic Peptide Facilitates Neutrophil Infiltration and Cardiac Matrix Metalloproteinase-9 Expression After Acute Myocardial Infarction

Rika Kawakami, MD; Yoshihiko Saito, MD, PhD; Ichiro Kishimoto, MD, PhD; Masaki Harada, MD, PhD; Koichiro Kuwahara, MD, PhD; Nobuki Takahashi, MD; Yasuaki Nakagawa, MD; Michio Nakanishi, MD; Keiji Tanimoto, MD; Satoru Usami, MD; Shinji Yasuno, MD; Hideyuki Kinoshita, MD; Hideki Chusho, MD, PhD; Naohisa Tamura, MD, PhD; Yoshihiro Ogawa, MD, PhD; Kazuwa Nakao, MD, PhD

Background—Recent clinical trials have shown that systemic infusion of nesiritide, a recombinant human brain natriuretic peptide (BNP), improves hemodynamic parameters in acutely decompensated hearts. This suggests that BNP exerts a direct cardioprotective effect and might thus be a useful therapeutic agent with which to treat acute myocardial infarction (MI). In the present study, we used BNP-transgenic (BNP-Tg) mice with elevated plasma BNP to determine whether and how BNP contributes to left ventricular remodeling and healing after MI.

Methods and Results—We examined the accumulation of neutrophils and the expression and activation of matrix metalloproteinase (MMP)-9 in the ventricles of male BNP-Tg mice and their nontransgenic (non-Tg) littermates during the early phase after acute MI. The numbers of neutrophils infiltrating the infarcted area were significantly increased in BNP-Tg mice 3 days after MI. In addition, both the gene expression and zymographic activity of MMP-9, but not MMP-2, were significantly higher in BNP-Tg than non-Tg mice. Double immunostaining revealed that neutrophils are the main source of the MMP-9, although doxycycline, an MMP inhibitor, had no effect on neutrophil infiltration of the infarcted area in BNP-Tg mice.

Conclusions—These results demonstrate that elevated plasma BNP facilitates neutrophil infiltration of the infarcted area after MI and increases the activity of the MMP-9 they produce. This suggests that BNP plays a key role in the processes of extracellular matrix remodeling and wound-healing during the early phase after acute MI. (***Circulation.*** **2004;110: 3306-3312.)**

Key Words: metalloproteinases ■ myocardial infarction ■ natriuretic peptides ■ remodeling ■ neutrophils

By secreting both atrial and brain natriuretic peptides (ANP and BNP, respectively), which act via natriuretic peptide receptor A (NPRA) to induce natriuresis, diuresis, and vasodilation and to inhibit the renin-angiotensin-aldosterone and sympathetic nervous systems, the heart serves as an important endocrine organ involved in the regulation of blood pressure and fluid-electrolyte balance.[1,2] ANP is synthesized and secreted primarily from the atria in adult mammals, whereas BNP is secreted primarily from the ventricle.[3] Synthesis and secretion of both ANP and BNP are markedly increased in patients with congestive heart failure.[4] Plasma BNP levels are also strongly increased during the early phase of acute myocardial infarction (MI), although plasma ANP levels are increased only slightly.[5] Such sustained increases in plasma BNP are correlated with enlargement of the left ventricle (LV), decreased ventricular contractility, and increased ventricular stiffness,[6,7] which suggests that BNP might play a significant role in ventricular remodeling. In fact, using BNP-deficient mice, we previously showed that endogenous BNP is a local regulator of ventricular fibrosis.[8]

Intravenous infusion of nesiritide, a recombinant human BNP, was recently reported to have beneficial hemodynamic effects in patients with decompensated congestive heart failure.[9,10] In addition to alleviating cardiac preload and afterloads, BNP might exert a direct cardioprotective effect[11,12] that could prevent LV remodeling after MI. The

Received January 4, 2004; de novo received June 8, 2004; accepted July 7, 2004.

From the Department of Medicine and Clinical Science, Kyoto University Graduate School of Medicine, Kyoto, Japan. Dr Saito is now at the First Department of Internal Medicine, Nara Medical University, Nara, Japan.

The online-only Data Supplement, which contains an additional figure, can be found with this article at http://www.circulationaha.org.

Correspondence to Ichiro Kishimoto, National Cardiovascular Center, 5-7-1 Fujishiro-dai, Suita, Osaka, 565-8565, Japan. E-mail kishimot@ri.ncvc.go.jp

Circulation **is available at http://www.circulationaha.org** **DOI: 10.1161/01.CIR.0000147829.78357.C5**

effects of continuously high levels of BNP on the infarcted myocardium are unknown, however. We therefore used BNP-transgenic (BNP-Tg) mice to investigate the effects of sustained increases in plasma BNP on cardiac repair pathways and remodeling after MI. These mice overexpress the BNP in their livers and show a >100-fold increase in plasma BNP levels throughout their lives.[13,14] In the present study, we focused on leukocyte infiltration, the genetic regulation of myocardial collagen synthesis including transforming growth factor (TGF)-β, and the activity of matrix metalloproteinase (MMP)-9, an important regulatory enzyme involved in extracellular matrix (ECM) degradation and cell migration during cardiac wound healing,[15,16] in infarcted BNP-Tg hearts.

Methods

Experimental Animals

BNP-Tg mice were developed as previously described[13] by use of the liver-specific human serum amyloid P component promoter. These mice show plasma BNP concentrations that are at least 2 orders of magnitude higher than those of their wild-type littermates, C57BL/6J nontransgenic (non-Tg) mice. Acute MI was induced in male BNP-Tg (n=51) and non-Tg (n=43) mice (age, 8 to 12 weeks; weight, 25 to 30 g) by ligation of the left coronary artery.[17,18] The same procedure without coronary artery ligation served as the sham operation. The experimental animals were monitored for 7 days after MI had been induced.

Echocardiography

Echocardiography was performed under light anesthesia with a mixture of ketamine (80 mg/kg) and xylazine (4 mg/kg) and spontaneous respiration.[19]

Hemodynamic and Infarct Size Measurements

After 3 days, a 2F Millar Micro-Tip catheter transducer (Millar Instruments) was inserted into the right carotid artery and then advanced into the LV for recording of LV systolic pressure, LV end-diastolic pressure, and LV maximum and minimum rates of pressure development (dP/dt). The ventricles were excised after evaluation of hemodynamic parameters. Infarct size was expressed as the ratio of the infarct to total LV mass as previously described.[17]

Immunohistochemistry and Quantitative Analysis of Histology

In a subset of animals (6 BNP-Tg and 6 non-Tg), the LV was cut into 3 transverse sections (apex, middle ring, and base) 3 days after MI. Immunostaining was then performed on frozen tissue specimens (6 μm) with rat anti-mouse 7/4 antibody (Serotec), which recognizes a polymorphic 40-kDa antigen expressed by neutrophils, and goat anti-mouse MMP-9 antibody (Santa Cruz Biotechnology). For each section, neutrophil 7/4-positive cells were counted in the infarcted area in at least 8 to 10 randomly selected high-power fields by use of a computer program (KS400 Version 3.00; Carl Zeiss).

Myeloperoxidase Activity Assay

Myeloperoxidase (MPO) activity was measured spectrophotometrically at 460 nm in 50 mmol/L phosphate buffer (pH 6.0) containing 0.167 mg/mL *o*-dianisidine hydrochloride (Sigma) and 0.0005% hydrogen peroxide as described previously.[20] One unit of MPO was defined as the quantity of enzyme needed to hydrolyze peroxide at a rate of 1 mmol/min at 25°C.

Northern Blot Analysis

Northern blots were made using 20 μg of total RNA isolated from frozen LV tissue by use of a technique described in detail elsewhere.[8] The probes for collagen I, collagen III, TGF-β_1, TGF-β_3, fibronectin and BNP were already available to us.[8] The other cDNA probes were prepared using reverse transcription–polymerase chain reaction with primers based on the published sequences.

Zymographic Measurement of Gelatinase Activity

MMP activity in 30 μg of myocardial extract was measured by gelatin zymography as previously described.[21,22] The gelatinolytic zones were quantified by use of NIH 1.62 image analysis software.[22]

Type IV Collagenase Activity Assay

The activity of type IV collagenases (MMP-2 and MMP-9) was assessed by use of a commercially available kit (Yagai Research Center) according to the manufacturer's instructions.[23]

Treatment With Doxycycline

In the doxycycline study, mice receiving 60 mg/kg doxycycline per day by gavage were compared with an untreated control group. Administration of doxycycline was started 3 days before induction of experimental MI and continued for 7 days after MI.

Data Analysis

All results are reported as mean±SEM. Two-way ANOVA followed by Tukey-Kramer tests was used to evaluate the effects of MI and genotype. The mortality data (deaths during the 7-day protocol, including causes of death) were analyzed by use of the χ^2 test. Values of $P<0.05$ were considered significant.

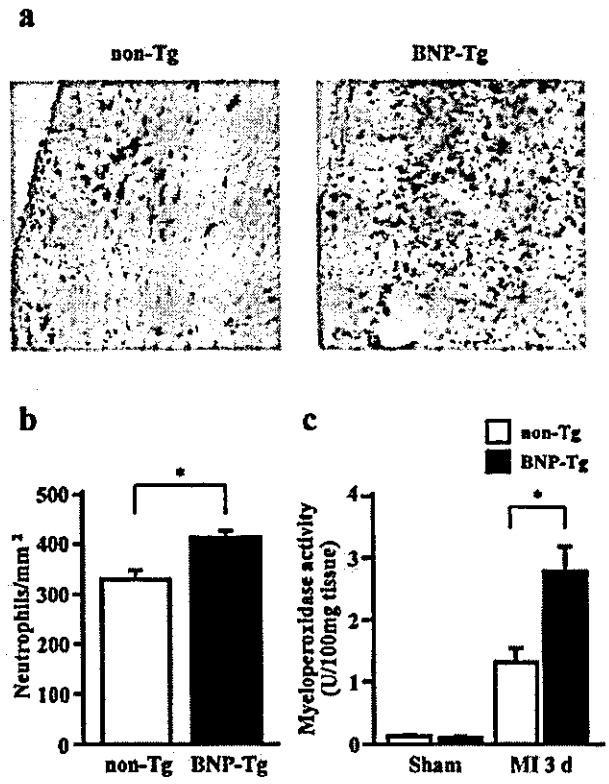

Figure 1. Accumulation of neutrophils in hearts of infarcted mice. a, Representative micrograph showing stained neutrophils within infarcted region (magnification ×200). b, Numbers of neutrophils per mm² within infarcted area 3 days after MI (n=6 for each). c, Cardiac MPO activity expressed as units/100 mg tissue wet wt in sham-operated and infarcted mice 3 days after MI (n=8 for each). Values are mean±SEM; *$P<0.01$ vs non-Tg mice with MI.

Echocardiographic and Hemodynamic Data

	Non-Tg		BNP-Tg	
	Sham	MI	Sham	MI
Echocardiographic data				
LV EDD, mm	4.4±0.1	4.8±0.1†§	4.3±0.1	4.8±0.1*§
LV ESD, mm	3.2±0.2	3.7±0.1*§	2.9±0.1	3.6±0.1‡
FS, %	31.7±1.7	23.5±1.9*§	31.2±1.5	25.6±2.3
Wall thickness, mm				
Infarct	N/A	0.70±0.03	N/A	0.61±0.02
Noninfarct	0.55±0.03	0.73±0.01†§	0.54±0.02	0.69±0.04*‡
Hemodynamic data				
LVSP, mmHg	100±3	68±2†	82±9*	69±2†
LV EDP, mmHg	4.8±0.4	6.0±0.5	4.4±0.7	5.8±0.5
+LV dP/dt_{max}, mm Hg/s	10 936±570	6433±545†‡	9200±1119	7133±492†
−LV dP/dt_{min}, mm Hg/s	10 836±784	6416±545†	9340±1386	7116±493†

Values are shown as mean±SEM. EDD indicates end-diastolic diameter; ESD, end-systolic diameter; FS, fractional shortening; N/A, not applicable; SP, systolic pressures; EDP, end-diastolic pressure; and dP/dt, maximum and minimal rate of pressure development.

*$P<0.5$, †$P<0.01$ vs sham-operated non-Tg mice.

‡$P<0.05$, §$P<0.01$ vs sham-operated BNP-Tg mice.

Results

Infarct Size, Echocardiography, and Hemodynamics

Three days after left coronary artery ligation, the sizes of the resultant infarcts were similar in BNP-Tg and non-Tg mice (BNP-Tg, 42.2±3.7% versus non-Tg, 40.4±3.8%; $P=0.75$, n=7). To evaluate the effect of a high plasma BNP concentration on the performance of the infarcted heart, we assessed cardiac function and LV geometry by use of echocardiography. The Table shows that the increase in LV chamber size and the noninfarcted wall thickness were the same in BNP-Tg and non-Tg mice 3 days after MI. LV systolic pressure measured by use of a Millar catheter was lower in sham-operated BNP-Tg mice than in sham-operated non-Tg mice (Table), which is consistent with our earlier observation that systolic blood pressure measured by use of the tail-cuff method was ≈20 mm Hg lower in BNP-Tg than non-Tg mice.[13] Conversely, there was no significant difference in LV systolic pressure, LV end-diastolic pressure, LV $+dP/dt_{max}$, or $-dP/dt_{min}$ between the 2 groups after ligation. We did, however, note a trend toward improved hemodynamic and echocardiographic parameters in BNP-Tg mice, although it did not reach statistical significance.

Infarct Infiltration by Neutrophils

Accumulation of leukocytes in the infarcted region is thought to be one step in the process of wound repair.[16,24] We therefore counted the leukocytes infiltrating the infarcted region after MI by use of a neutrophil-specific antibody. Neutrophils were identified throughout the infarcted segments after MI (Figure 1a). Moreover, although quantitative analysis of images of the infarcted region obtained 3 days after MI showed that their numbers increased in both BNP-Tg and non-Tg mice, there were significantly greater numbers of neutrophils in BNP-Tg than non-Tg hearts (BNP-Tg, 415.41±12.90 cells/mm^2 versus non-Tg, 330.70±16.82 cells/mm^2; $P<0.01$, n=6; Figure 1b).

To further assess neutrophil accumulation in the infarcted areas, we also measured MPO activity. As shown in Figure 1c, cardiac MPO activity was significantly higher in BNP-Tg than non-Tg mice 3 days after MI (BNP-Tg, 2.80±0.40 U/100 mg tissue versus non-Tg, 1.33±0.23 U/100 mg tissue; n=8 to 10, $P<0.01$), whereas there was no difference between the sham-operated groups.

Taken together, the data presented in this section clearly indicate that within 3 days after MI, neutrophils accumulate to a significantly greater degree in the infarcted regions of BNP-Tg hearts than non-Tg hearts.

Cardiac Gene Expression in Infarcted Hearts

Recent evidence highlights the involvement of the plasminogen activator–metalloproteinase system in myocardial neutrophil accumulation, the repair processes, and the rupture seen after MI.[15,16] When we examined gene expression of plasminogen activators and MMPs 3 days after MI, we found that, with the exception of GAPDH, transcription of all the genes examined was upregulated compared with sham-operated animals. In addition, expression of MMP-9 mRNA was significantly higher in BNP-Tg than non-Tg mice after ligation (Figure 2, a and b), whereas there was no difference in the expression of MMP-2, TIMP-1, urokinase-type plasminogen activator, and plasminogen activator inhibitor-1 mRNA in the 2 MI groups.

We also focused on the synthetic processes involved in collagen turnover by examining the expression of mRNAs encoding TGF-β_1, TGF-β_3, collagen I, and collagen III, which are known to be involved in cardiac fibroblast proliferation and the biosynthesis of ECM proteins.[25–27] We found that their expression was similarly upregulated in the infarcted regions of both BNP-Tg and non-Tg hearts (Figure 2, a and b), indicating that overexpression of BNP does not affect the biosynthesis of collagen during the early phase of acute MI.

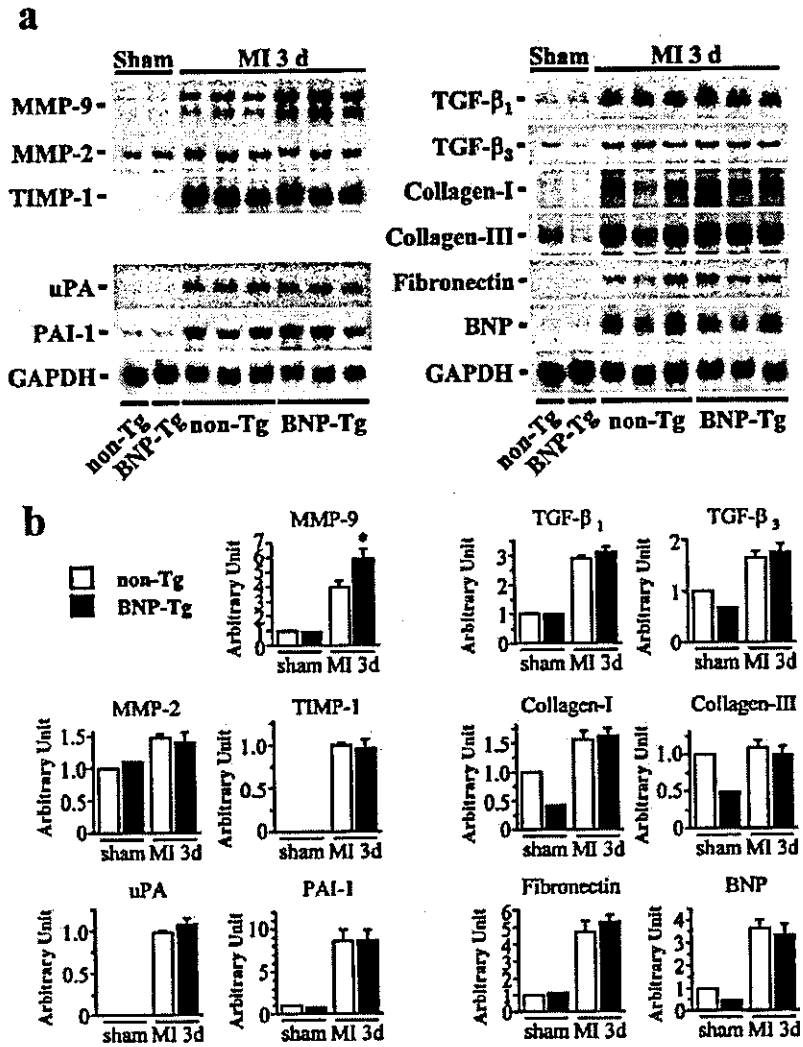

Figure 2. a, Representative autoradiograms showing Northern blot analysis in hearts harvested from sham-operated and infarcted mice 3 days after MI. b, Summary of results obtained from Northern blot analyses; mRNA levels in sham-operated non-Tg hearts were assigned a value of 1.0. Values are mean±SEM; *$P<0.05$ vs non-Tg mice with MI.

Increased MMP Activity in Infarcted Hearts

We next used gelatin zymography to evaluate the extent to which overexpression of BNP affects MMP-9 enzymatic activity. As shown in Figure 3a, the gelatinase activity of MMP-9, but not MMP-2, was significantly ($P<0.05$) elevated in infarcted BNP-Tg hearts compared with infarcted non-Tg hearts. Likewise, type IV collagenase activity was significantly higher in infarcted BNP-Tg than non-Tg hearts

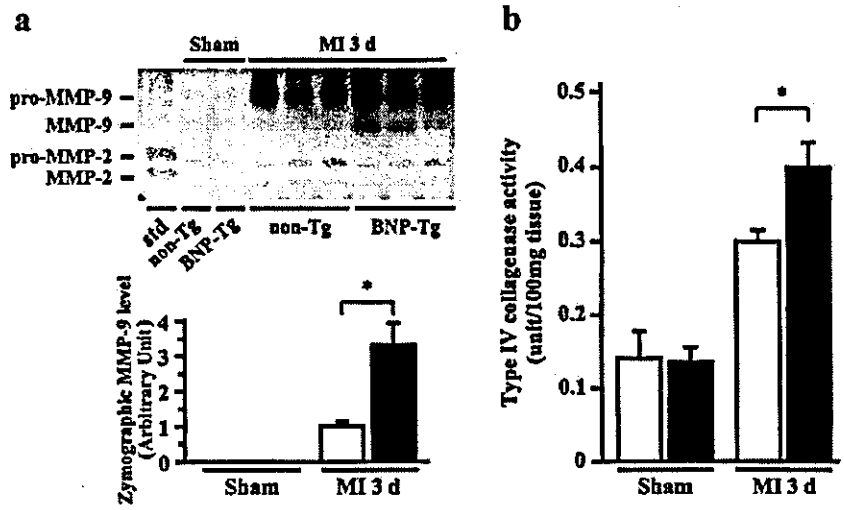

Figure 3. a, Top, Representative gelatin zymography performed 3 days after MI (n=6 for each); a mixture of human MMP-2 and pro-MMP-9 served as a standard (std). Bottom, densitometric analysis of MMP-9 abundance. b, Cardiac type IV collagenase activity expressed as units/100 mg tissue wet weight 3 days after MI (n=7 for each). Values are mean±SEM; *$P<0.05$ vs non-Tg mice with MI.

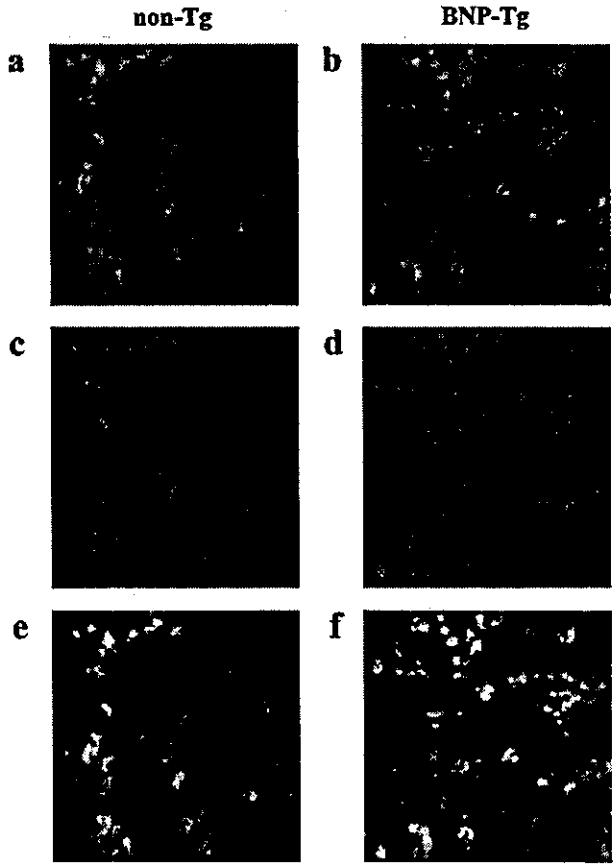

Figure 4. Confocal images of double immunostaining for MMP-9 and neutrophil 7/4. Immunostaining and cellular localization of MMP-9 within infarcted hearts of BNP-Tg (right) and non-Tg (left) mice 3 days after MI. Images show single immunostaining for MMP-9 (green) (a and b) and neutrophil 7/4 (red) (c and d). Double immunostaining (yellow) shows colocalization of MMP-9 within 7/4-stained neutrophils in infarcted region after MI (e and f). Magnification ×400.

(BNP-Tg, 0.399±0.037 U/100 mg wet wt versus non-Tg, 0.300±0.017 U/100 mg wet wt; n=7, $P<0.05$; Figure 3b). Because MMP-9 and -2 are the 2 major collagenases that degrade type IV collagen[23] and zymography showed that there was no difference in MMP-2 activity within the infarcts of BNP-Tg and non-Tg mice, the increased digestion of type IV collagen in BNP-Tg hearts is attributable to the increase in MMP-9 activity.

Neutrophils Are the Predominant Source of MMP-9

We then evaluated the distribution of the MMP-9 by using confocal fluorescence microscopy to visualize the double immunostaining of MMP-9 (green) and neutrophils (red) in thin sections of frozen mouse LV. Three days after MI, immunoreactive MMP-9 and neutrophils were detected within the infarcted myocardium and the border regions in both BNP-Tg and non-Tg hearts (Figure 4, a–d). Moreover, the double labeling revealed that the distribution of immunoreactive neutrophils overlapped that of MMP-9 (Figure 4, e and f), indicating that the major source of MMP-9 is the neutrophils infiltrating the infarcted region. By contrast, MMP-9 levels were negligible in the sham-operated mice and the noninfarcted regions of the infarcted mice (data not shown).

MMP-9 Inhibition Did Not Affect Neutrophil Infiltration in BNP-Tg

Finally, we assessed the functional significance of MMPs in BNP-Tg mice subjected to experimental MI by treating the mice with doxycycline, a nonselective MMP inhibitor. We found that the numbers of neutrophils detected by use of anti-mouse neutrophil 7/4 antibody were similarly increased in control BNP-Tg and doxycycline-treated BNP-Tg mice (control BNP-Tg, 428.24±29.84 cells/mm^2 versus doxycycline-treated BNP-Tg, 432.93±23.86 cells/mm^2; $P=0.90$, n=6; Figure 5, a and b). Likewise, there were no significant differences in the cardiac MPO activity in control BNP-Tg and doxycycline-treated BNP-Tg mice (control BNP-Tg, 3.03±0.36 U/100 mg tissue versus doxycycline-treated BNP-Tg, 2.80±0.32 U/100 mg tissue; $P=0.63$; Figure 5c). Thus, the increased infiltration of neutrophils into the infarcted area was not dependent on increased MMP-9 activity in the neutrophils themselves.

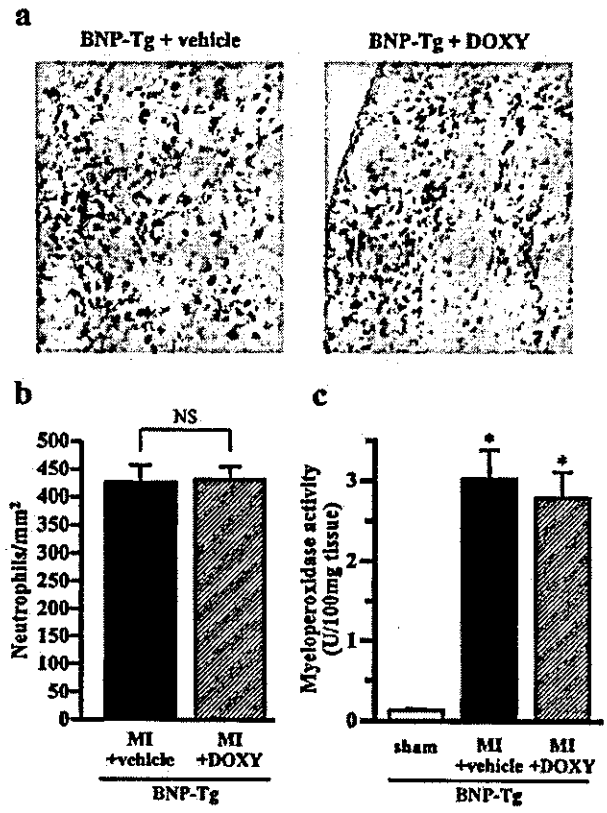

Figure 5. Accumulation of neutrophils within infarcted regions of control BNP-Tg and doxycycline-treated BNP-Tg mice. a, Representative micrograph showing stained neutrophils within infarct area (magnification ×200). b, Numbers of neutrophils per mm^2 within infarcted area 3 days after MI (n=6 for each). Values are shown as mean±SEM; NS, not significant. c, Cardiac MPO activity expressed as units/100 mg tissue wet weight in sham-operated (n=3 for each), untreated infarcted (n=18), and doxycycline-treated infarcted BNP-Tg mice (n=17). Values are mean±SEM; *$P<0.01$ vs sham values.

Discussion

We previously showed that plasma BNP levels are greatly elevated in patients with acute MI; they reach a peak within 24 hours after onset, then decline and increase again to a second peak over the next 3 to 7 days.[5] Thus, high plasma BNP levels persist during the period when neutrophils and other inflammatory cells infiltrate the infarcted area. In the present study, we used BNP-Tg mice to assess the effects of a pharmacological dose of BNP on the myocardium early after acute MI. We found that (1) there is a greater accumulation of neutrophils in BNP-Tg hearts; (2) gene expression and enzyme activity of MMP-9 are higher in BNP-Tg hearts; (3) the major source of MMP-9 is the neutrophils infiltrating the infarcted region of BNP-Tg hearts; and (4) doxycycline, a potent MMP inhibitor, has no effect on the increased infiltration of neutrophils into the infarcted area in BNP-Tg mice.

The wound repair process involves temporally overlapping phases that include inflammation, new tissue formation, and tissue remodeling.[28] During the inflammatory phase, collagen and other ECM components may be degraded as a result of increased MMP activity.[29,30] In the present study, we found that early after MI, neutrophil infiltration of the infarcted area is augmented in BNP-Tg mice, and that there are corresponding increases in MMP-9 expression and activity associated with the infiltrating neutrophils. By contrast, there were no significant changes in the levels of TGF-β_1, TGF-β_3, collagen I, collagen III, or fibronectin mRNA, which suggests that overexpression of BNP leads to exaggerated collagen degradation by MMP-9 produced by neutrophils without an apparent increase in synthesis. Moreover, the fact that the increase in zymographic MMP-9 activity in BNP-Tg mice appeared to be more pronounced than the increase in neutrophil number suggests that BNP may have a direct effect on the amount of MMP-9 activity produced by each activated neutrophil. This idea is supported by the results of supplemental experiments showing that in the presence of the neutrophil-activating factor formyl-methionyl-leucyl-phenylalanine (fMLP; 10^{-7} mol/L), ANP (10^{-8} mol/L), which shares its receptor (NPRA) with BNP and is equally potent, elicited a 2.1-fold increase ($P<0.01$) in the transcription and activation of MMP-9 in human neutrophils.

We also tested whether upregulation of MMP-9 contributes to the accumulation of neutrophils in BNP-Tg mice. On the basis of evidence that it suppresses the activity of such MMPs as collagenase, gelatinase, and stromelysin both directly and indirectly,[31] we used doxycycline to evaluate the extent to which elevated MMP production is involved in neutrophil accumulation within the infarcted regions of BNP-Tg hearts. That we found no difference in the neutrophil accumulation in control BNP-Tg and doxycycline-treated BNP-Tg mice suggests that the increased MMP-9 activity is most likely not responsible for the neutrophil accumulation in BNP-Tg animals. Conversely, one possible explanation for the increased leukocyte infiltration is that BNP exerts a direct effect on neutrophil chemotaxis. In fact, a recent study has shown that ANP affects human neutrophil migration at concentrations ranging from 4×10^{-9} to 10^{-7} mol/L.[32] The plasma BNP concentration in BNP-Tg mice was approximately 3×10^{-9} mol/L, which is comparable to the effective ANP concentration reported earlier, because ANP and BNP act via NPRA with equal potency. Another possible explanation is an indirect effect via endothelial adhesion molecules. We previously showed that the diminished neutrophil accumulation seen during ischemia/reperfusion in NPRA-deficient mice is probably a result of suppressed expression of P-selectin in coronary endothelial cells and that ANP upregulates P-selectin expression in cultured endothelial cells exposed to oxidative stress.[20] Thus, BNP might increase neutrophil accumulation by upregulating one or more of the endothelial adhesion molecules that tether circulating neutrophils to the endothelium.

Heymans et al[16] recently showed that MMP-9 deficiency retards the wound healing process after MI in mice, which increases the size of residual necrotic areas. In the same study, these investigators also showed that the lack of MMP-9 proteolytic activity results in almost complete protection against infarct rupture. These results suggest that MMP-9 is a key regulator of infarct healing and rupture, acting via degradation of ECM early after acute MI. Indeed, BNP-Tg mice tended to die of cardiac rupture more frequently than non-Tg mice: among the dead mice (26 BNP-Tg and 9 non-Tg), 47.1% (n=24) of the BNP-Tg mice died of cardiac rupture after MI, whereas 18.6% (n=2) of non-Tg mice died of the same cause ($P=0.75$ by χ^2 analysis). Moreover, although the effect did not reach statistical significance, doxycycline tended to attenuate cardiac rupture in BNP-Tg mice, suggesting that elevated MMP-9 activity may be involved. However, because the level of collagen and TGF-β expression is lower in sham-operated BNP-Tg hearts than in sham-operated non-Tg hearts (Figure 2), the apparent high frequency of cardiac rupture in BNP-Tg mice might be attributable to a reduction in collagen matrix in BNP-Tg mice. More importantly, the transient activation of MMP-9 induced by BNP may speed up infarct healing and modulate the overall late remodeling process. In fact, at 6 weeks after ligation, LV dilatation and hypertrophy of the noninfarcted zone seen in the non-Tg mice are attenuated in BNP-Tg mice (our unpublished data). These observations suggest that transient MMP-9 expression induced by the elevation in BNP during the earliest phase after MI is a cardioprotective mechanism affecting late LV remodeling.

In summary, overexpression of BNP in mice led to neutrophil infiltration and MMP-9 expression in the infarcted region after MI, an effect that could lead to exaggerated degradation of ECM components. This suggests that BNP plays a novel role in the process of cardiac repair during the acute phase of MI.

Acknowledgments

This work was supported in part by research grants from the Japanese Ministry of Education, Science, and Culture; the Japanese Ministry of Health and Welfare; and the Japanese Society for the Promotion of Science Research for the Future program (JSPS-RFTF96I00204 and JSPS-RFTF98L00801). Excellent secretarial work by K. Okamura is also acknowledged.

References

1. De Bold AJ. Atrial natriuretic factor: a hormone produced by the heart. *Science*. 1985;230:767–770.

2. Rosenzweig A, Seidman CE. Atrial natriuretic factor and related peptide hormones. *Annu Rev Biochem.* 1991;60:229–255.
3. Mukoyama M, Nakao K, Hosoda K, et al. Brain natriuretic peptide as a novel cardiac hormone in humans: evidence for an exquisite dual natriuretic peptide system, atrial natriuretic peptide and brain natriuretic peptide. *J Clin Invest.* 1991;87:1402–1412.
4. Mukoyama M, Nakao K, Saito Y, et al. Increased human brain natriuretic peptide in congestive heart failure. *N Engl J Med.* 1990;323:757–758.
5. Morita E, Yasue H, Yoshimura M, et al. Increased plasma levels of brain natriuretic peptide in patients with acute myocardial infarction. *Circulation.* 1993;88:82–91.
6. Yamamoto K, Burnett JC Jr, Jougasaki M, et al. Superiority of brain natriuretic peptide as a hormonal marker of ventricular systolic and diastolic dysfunction and ventricular hypertrophy. *Hypertension.* 1996; 28:988–994.
7. Nagaya N, Goto Y, Nishikimi T, et al. Sustained elevation of plasma brain natriuretic peptide levels associated with progressive ventricular remodelling after acute myocardial infarction. *Clin Sci.* 1999;96: 129–136.
8. Tamura N, Ogawa Y, Chusho H, et al. Cardiac fibrosis in mice lacking brain natriuretic peptide. *Proc Natl Acad Sci U S A.* 2000;97:4239–4244.
9. Mills RM, LeJemtel TH, Horton DP, et al. Sustained hemodynamic effects of an infusion of nesiritide (human b-type natriuretic peptide) in heart failure: a randomized, double-blind, placebo-controlled clinical trial. Natrecor Study Group. *J Am Coll Cardiol.* 1999;34:155–162.
10. Colucci WS, Elkayam U, Horton DP, et al. Intravenous nesiritide, a natriuretic peptide, in the treatment of decompensated congestive heart failure. Nesiritide Study Group. *N Engl J Med.* 2000;343:246–253.
11. Holtwick R, van Eickels M, Skryabin BV, et al. Pressure-independent cardiac hypertrophy in mice with cardiomyocyte-restricted inactivation of the atrial natriuretic peptide receptor guanylyl cyclase-A. *J Clin Invest.* 2003;111:1399–1407.
12. Molkentin J. A friend within the heart: natriuretic peptide receptor signaling. *J Clin Invest.* 2003;111:1275–1277.
13. Ogawa Y, Itoh H, Tamura N, et al. Molecular cloning of the complementary DNA and gene that encode mouse brain natriuretic peptide and generation of transgenic mice that overexpress the brain natriuretic peptide gene. *J Clin Invest.* 1994;93:1911–1921.
14. Chusho H, Ogawa Y, Tamura N, et al. Genetic models reveal that brain natriuretic peptide can signal through different tissue-specific receptor-mediated pathways. *Endocrinology.* 2000;141:3807–3813.
15. Creemers E, Cleutjens J, Smits J, et al. Disruption of the plasminogen gene in mice abolishes wound healing after myocardial infarction. *Am J Pathol.* 2000;156:1865–1873.
16. Heymans S, Luttun A, Nuyens D, et al. Inhibition of plasminogen activators or matrix metalloproteinases prevents cardiac rupture but impairs therapeutic angiogenesis and causes cardiac failure. *Nat Med.* 1999;5: 1135–1142.
17. Michael LH, Entman ML, Hartley CJ, et al. Myocardial ischemia and reperfusion: a murine model. *Am J Physiol.* 1995;269:H2147–H2154.
18. Patten RD, Aronovitz MJ, Deras-Mejia L, et al. Ventricular remodeling in a mouse model of myocardial infarction. *Am J Physiol.* 1998;274: H1812–H1820.
19. Ichihara S, Senbonmatsu T, Price E Jr, et al. Targeted deletion of angiotensin II type 2 receptor caused cardiac rupture after acute myocardial infarction. *Circulation.* 2002;106:2244–2249.
20. Izumi T, Saito Y, Kishimoto I, et al. Blockade of the natriuretic peptide receptor guanylyl cyclase-A inhibits NF-kappaB activation and alleviates myocardial ischemia/reperfusion injury. *J Clin Invest.* 2001;108: 203–213.
21. Silvestre JS, Mallat Z, Tamarat R, et al. Regulation of matrix metalloproteinase activity in ischemic tissue by interleukin-10: role in ischemia-induced angiogenesis. *Circ Res.* 2001;89:259–264.
22. Cho A, Reidy MA. Matrix metalloproteinase-9 is necessary for the regulation of smooth muscle cell replication and migration after arterial injury. *Circ Res.* 2002;91:845–851.
23. Fujimura M, Gasche Y, Morita-Fujimura Y, et al. Early appearance of activated matrix metalloproteinase-9 and blood-brain barrier disruption in mice after focal cerebral ischemia and reperfusion. *Brain Res.* 1999;842: 92–100.
24. Jugdutt BI. Ventricular remodeling after infarction and the extracellular collagen matrix: when is enough enough? *Circulation.* 2003;108: 1395–1403.
25. Weber KT, Brilla CG. Pathological hypertrophy and cardiac interstitium: fibrosis and renin- angiotensin-aldosterone system. *Circulation.* 1991;83: 1849–1865.
26. Butt RP, Laurent GJ, Bishop JE. Mechanical load and polypeptide growth factors stimulate cardiac fibroblast activity. *Ann N Y Acad Sci.* 1995;752: 387–393.
27. Cleutjens JP, Verluyten MJ, Smiths JF, et al. Collagen remodeling after myocardial infarction in the rat heart. *Am J Pathol.* 1995;147:325–338.
28. Singer AJ, Clark RA. Cutaneous wound healing. *N Engl J Med.* 1999; 341:738–746.
29. Etoh T, Joffs C, Deschamps A, et al. Myocardial and interstitial matrix metalloproteinase activity after acute myocardial infarction in pigs. *Am J Physiol.* 2001;281:H987–H994.
30. Tao ZY, Cavasin MA, Yang F, et al. Temporal changes in matrix metalloproteinase expression and inflammatory response associated with cardiac rupture after myocardial infarction in mice. *Life Sci.* 2004;74: 1561–1572.
31. Golub LM, Lee HM, Ryan ME, et al. Tetracyclines inhibit connective tissue breakdown by multiple non-antimicrobial mechanisms. *Adv Dent Res.* 1998;12:12–26.
32. Elferink JG, De Koster BM. Atrial natriuretic factor stimulates migration by human neutrophils. *Eur J Pharmacol.* 1995;288:335–340.

Clin Exp Immunol 2004; 137:430–436 doi:10.1111/j.1365-2249.2004.02534.x

Osteoprotegerin (OPG) acts as an endogenous decoy receptor in tumour necrosis factor-related apoptosis-inducing ligand (TRAIL)-mediated apoptosis of fibroblast-like synovial cells

T. MIYASHITA*, A. KAWAKAMI*, T. NAKASHIMA†, S. YAMASAKI*, M. TAMAI*, F. TANAKA*, M. KAMACHI*, H. IDA*, K. MIGITA*, T. ORIGUCHI‡, K. NAKAO§ & K. EGUCHI* *The First Department of Internal Medicine, Nagasaki University School of Medicine, Nagasaki, Japan, †Department of Hospital Pharmacy, Nagasaki University School of Medicine, Nagasaki, Japan, ‡Department of Physical Therapy, Nagasaki University School of Health Sciences, Nagasaki, Japan, and §Health Research Center, Nagasaki University, Nagasaki, Japan

(Accepted for publication 10 May 2004)

SUMMARY

We examined the role of osteoprotegerin (OPG) on tumour necrosis factor-related apoptosis-inducing ligand (TRAIL)-induced apoptosis in rheumatoid fibroblast-like synovial cells (FLS). OPG protein concentrations in synovial fluid from patients with rheumatoid arthritis (RA) correlated with those of interleukin (IL)-1β or IL-6. A similar correlation was present between IL-1β and IL-6 concentrations. Rheumatoid FLS *in vitro* expressed both death domain-containing receptors [death receptor 4 (DR4) and DR5] and decoy receptors [decoy receptor 1 (DcR1) and DcR2]. DR4 expression on FLS was weak compared with the expression of DR5, DcR1 and DcR2. Recombinant TRAIL (rTRAIL) rapidly induced apoptosis of FLS. DR5 as well as DR4 were functional with regard to TRAIL-mediated apoptosis induction in FLS; however, DR5 appeared be more efficient than DR4. In addition to soluble DR5 (sDR5) and sDR4, OPG administration significantly inhibited TRAIL-induced apoptogenic activity. OPG was identified in the culture supernatants of FLS, and its concentration increased significantly by the addition of IL-1β in a time-dependent manner. Neither IL-6 nor tumour necrosis factor (TNF)-α increased the production of OPG from FLS. TRAIL-induced apoptogenic activity towards FLS was reduced when rTRAIL was added without exchanging the culture media, and this was particularly noticeable in the IL-1β-stimulated FLS culture; however, the sensitivity of FLS to TRAIL-induced apoptosis itself was not changed by IL-1β. Interestingly, neutralization of endogenous OPG by adding anti-OPG monoclonal antibody (MoAb) to FLS culture restored TRAIL-mediated apoptosis. Our data demonstrate that OPG is an endogenous decoy receptor for TRAIL-induced apoptosis of FLS. In addition, IL-1β seems to promote the growth of rheumatoid synovial tissues through stimulation of OPG production, which interferes with TRAIL death signals in a competitive manner.

Keywords fibroblast-like synovial cells IL-1β OPG rheumatoid arthritis TRAIL

INTRODUCTION

The soluble receptor, osteoprotegerin (OPG), is a member of the tumour necrosis factor receptor (TNFR) superfamily and acts as a receptor antagonist. The decoy function of OPG towards receptor activator of nuclear factor κB ligand (RANKL) is well recognized; OPG binds RANKL, and thus prevents the interaction with, and stimulation of, RANK [1–3]. Hence, OPG inhibits osteoclast differentiation and survival as demonstrated both *in vivo* and *in vitro* [4]. OPG is also thought to be involved in inflammatory diseases based on results of experimental studies demonstrating stimulation of OPG production from endothelial cells by tumour necrosis factor (TNF)-α and interleukin (IL)-1β [5]. Furthermore, OPG has also been shown to exhibit mitogenic and/or anti-apoptotic properties for foreskin fibroblasts and/or endothelial cells [6,7].

Marked hyperplasia of synovial tissues is a characteristic feature of rheumatoid arthritis (RA), which is mediated, at least in part, by impaired apoptosis of synovial cells *in situ* [8]. The anti-apoptotic feature of rheumatoid synovial cells *in situ* may not be intrinsic, but rather develop in the inflammatory rheumatoid microenvironment. In this regard, we have demonstrated that the sensitivity of fibroblast-like synovial cells (FLS) to apoptogenic

Correspondence: Katsumi Eguchi MD, The First Department of Internal Medicine, Nagasaki University School of Medicine, 1-7-1 Sakamoto, Nagasaki 852–8501, Japan.
E-mail: eguchi@net.nagasaki-u.ac.jp

stimuli is modulated by various inflammatory cytokines [9–11]. OPG acts also as a receptor antagonist for TNF-related apoptosis-inducing ligand (TRAIL) [12]. We have shown recently that FLS are sensitive toward TRAIL-mediated apoptosis [13]. TRAIL triggers the activation of caspase-8 in FLS, which induces mitochondrial perturbation [13]. As both mitochondrial perturbation and DNA fragmentation were completely inhibited by caspase-8 inhibitor, FLS are classed into type II cell death in response to TRAIL [13]. The regulatory mechanisms of inflammatory cytokines on OPG production may influence TRAIL-induced apoptosis of synovial cells, and thus defines a new functional role for OPG in the pathological process of RA.

In the present study, we demonstrate that IL-1β in rheumatoid synovial fluid is the major inflammatory cytokine responsible for stimulation of OPG synthesis from FLS. Furthermore, our data suggest that OPG produced by FLS is an endogenous receptor antagonist of TRAIL-induced apoptosis in FLS which may, in part, explain the growth-promoting activity of IL-1β for rheumatoid synovial tissues.

MATERIALS AND METHODS

Determination of OPG, IL-1β, IL-6 and TNF-α concentrations in synovial fluid from patients with RA

Synovial fluid samples were obtained from patients with RA, who fulfilled the criteria of the American Rheumatism Association for RA [14], admitted to the National Ureshino Hospital (28 synovial fluid samples from 28 RA patients). The experimental protocol was approved by the Hospital Human Ethics Review Committee and signed consent was obtained from each patient. The concentrations of OPG, IL-1β, IL-6 and TNF-α in the rheumatoid synovial fluid were examined by a sandwich enzyme-linked immunosorbent assay (ELISA) (OPG; Immunodiagnostik AC, Bensheim, Germany: IL-1β, IL-6 and TNF-α; Otsuka Pharmaceutical Co., Tokushima, Japan). In brief, the plates precoated with monoclonal antibody (MoAb) against OPG, IL-1β, IL-6 or TNF-α were incubated with the samples, incubated further with the secondary antibody, and colour was developed according to the protocol provided by the supplier.

Effect of inflammatory cytokines on OPG production from cultured FLS

FLS were isolated from 20 patients with RA at the time of orthopaedic surgery (total knee replacement) conducted at National Ureshino Hospital. Signed consent was also obtained from each patient. Briefly, the synovial tissues were trimmed of fat and minced with scissors, then added to a mixture of collagenase (Sigma Chemical Co., St Louis, MO, USA) and dispase (Godo Shusei Co., Tokyo). The tissue mixture was digested over a 45-min period during gentle stirring at 37°C, and the harvested cells were allowed to adhere to Petri dishes (Falcon 3003, Becton Dickinson Co., Oxnard, CA, USA). The adherent cells used in the present study at third to fifth passages were less than 1% reactive with various MoAbs, including CD3, CD68, CD20 and von-Willebrand factor, which define FLS. Isolated FLS were cultured in the presence or absence of recombinant IL-1β (rIL-1β, Otsuka Pharmaceutical Co., 20 IU/ml), rIL-6 plus r-soluble IL-6 receptor (sIL-6R) (R&D Systems Inc., Minneapolis, MN, USA, 100 ng/ml each) or rTNF-α (R&D Systems, 200 IU/ml) for indicated time intervals in RPMI-1640 containing 10% fetal calf serum (FCS) (1×10^5/35 mm dish). OPG protein concentration in the culture supernatants was examined by the sandwich ELISA as described above.

Expression of TRAIL receptors on cultured FLS

Expression of TRAIL receptors on cultured rheumatoid FLS was examined by flow cytometric analysis. Treated FLS were detached by addition of 0·265 mM EDTA, washed with phosphate buffered saline (PBS) and incubated with antihuman death receptor 4 (DR4; R&D Systems), antihuman DR5 (R&D Systems), antihuman decoy receptor 1 (DcR1; R&D Systems) or antihuman DcR2 (R&D Systems) at 4°C for 30 min. After incubation, the cells were washed with PBS, incubated further with phycoerythrin (PE)-conjugated antigout IgG (Sigma Chemical Co.), and the expression of DR4, DR5, DcR1 and DcR2 was examined by flowcytometer (Epics XL, Beckman Coulter, Hialeah, FL, USA).

Effect of OPG toward TRAIL-induced apoptosis of cultured FLS

We have shown recently that cultured FLS are committed to type II cell death in response to TRAIL [13], thus disruption of

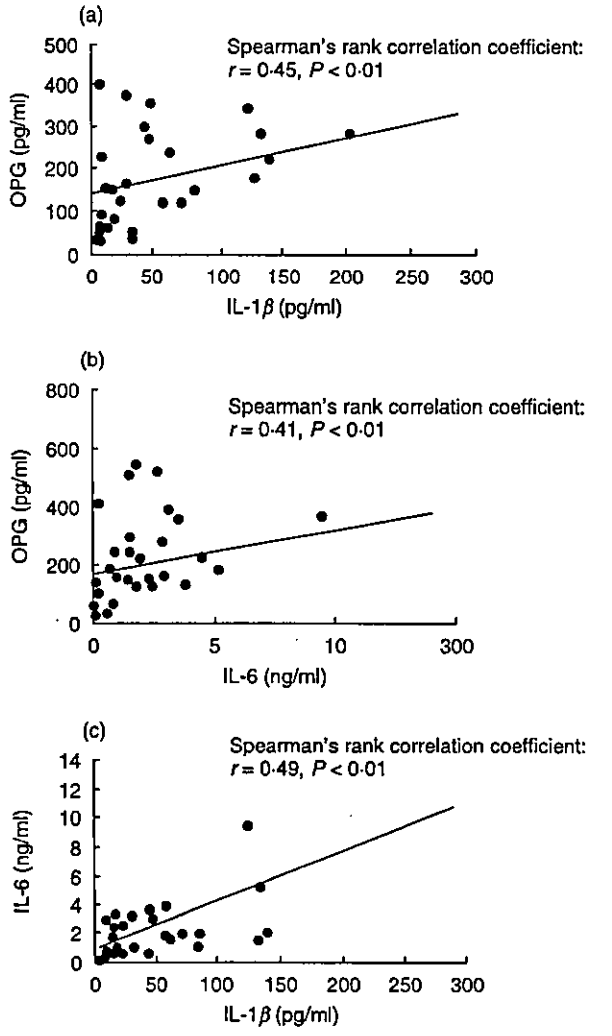

Fig. 1. Positive correlation of protein concentration between OPG and IL-1β (a), OPG and IL-6 (b) and IL-1β and IL-6 (c) found in synovial fluid samples (total 27 synovial fluids examined) of RA patients.

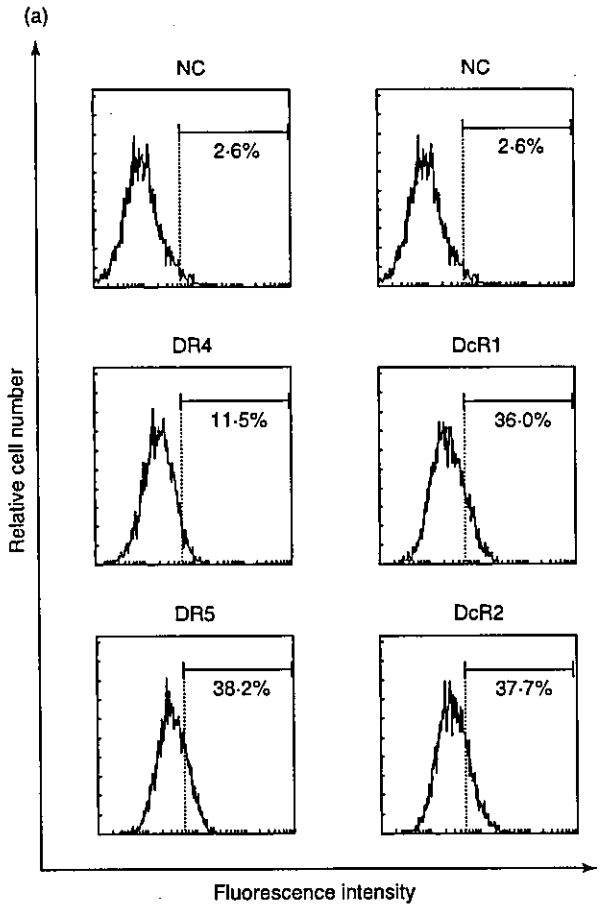

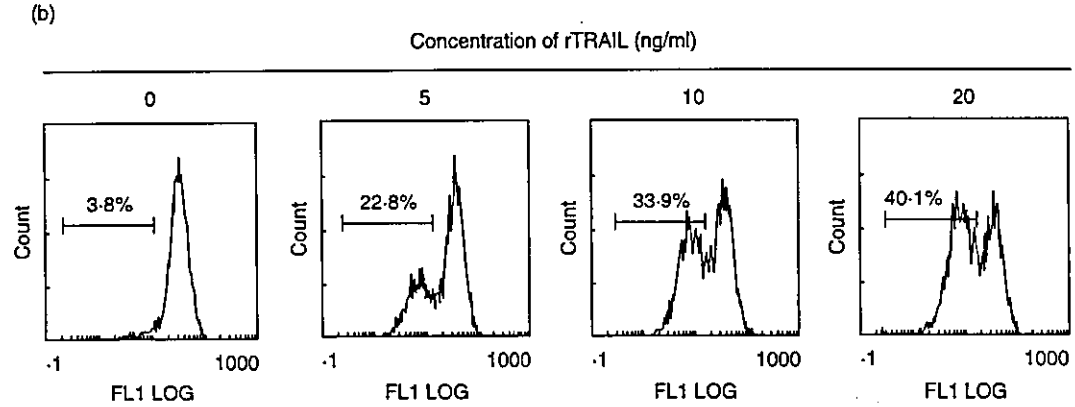

Fig. 2. TRAIL-mediated apoptosis in FLS by rTRAIL. (a) Expression of TRAIL receptors on FLS. Rheumatoid FLS were detached by adding EDTA, reacted with anti-DR4, anti-DR5, anti-DcR1 or anti-DcR2 at 4°C for 30 min, and incubated further with PE-conjugated antigout IgG at 4°C for 30 min. After incubation, surface expression of DR4, DR5, DcR1 and DcR2 on FLS was examined by flow cytometer as described in the text. Note that FLS expressed DR4, DR5, DcR1 and DcR2; however, DR4 expression was weak compared with the other three receptors. NC; negative control, stained with goat IgG instead of first antibody. Numbers are the percentage of positive cells. Results are representative data from five individual samples. (b) Quantification of TRAIL-mediated apoptosis in FLS by $\Delta\Psi m$. FLS were incubated with varying concentrations of rTRAIL for 2 h, detached by adding 0·265 mM EDTA, and $\Delta\Psi m$ was quantified as described in the text. Note that rTRAIL induced $\Delta\Psi m$ in FLS in a dose-dependent manner. Numbers are the percentage of positive cells. Results are representative data from five individual samples.

mitochondrial transmembrane potential ($\Delta\Psi m$) was used to quantify TRAIL-mediated FLS apoptosis in the present study. FLS were cultured in the presence or absence of various cytokines for indicated hours, washed, and incubated further with varying concentrations of rTRAIL (R&D Systems) with or without rOPG (R&D Systems), soluble DR4 (sDR4; R&D Systems) or sDR5 (R&D Systems) for an additional 2 h. After incubation, $\Delta\Psi m$ was examined as described recently [13]. In brief, treated FLS were detached by adding 0·265 mM EDTA, washed, and incubated further with a saturating amount of DiOC6 (3,3′-dihexyloxacarbocyamine iodide, Fluoreszenztechnologie, Grottenhofstr, Austria) at 37°C for 15 min. After incubation, the percentage of $\Delta\Psi m$ in FLS was quantified by flow cytometer (Epics XL, Beckman Coulter).In some experiments, rTRAIL was added to FLS culture without exchanging the culture media, and TRAIL-induced apoptosis in FLS was also examined by $\Delta\Psi m$. To neutralize endogenous OPG secreted from FLS in culture, anti-OPG MoAb (mouse IgG1; R&D Systems) was added, and TRAIL-mediated apoptosis in FLS was examined by $\Delta\Psi m$.

Statistical analysis

Statistical analyses were performed using the Student's *t*-test or Spearman's rank correlation analysis. *P*-values <0·05 were selected as the level of significance.

RESULTS

Determination of OPG protein in synovial fluid of patients with RA

First, we examined whether OPG protein was present in the rheumatoid synovial fluid. As reported recently [15,16], OPG protein was detected in all samples examined, although the level varied from one sample to another (Fig. 1a). Furthermore, there was a positive correlation between the concentrations of OPG and IL-1β. In addition, a similar correlation was demonstrated between the protein concentration of OPG and IL-6, and between that of IL-1β and IL-6 (Fig. 1b,c). In contrast, TNF-α was detected in only a proportion of the samples, and the levels of this cytokine did not correlate with OPG concentration (data not shown).

TRAIL induces apoptosis in FLS through DR4 and DR5

As shown in Fig. 2a, rheumatoid FLS *in vitro* expressed DR4, DR5, DcR1 and DcR2. Expression of DR4 was not so obvious compared with DR5, DcR1 and DcR2. Figure 2B shows that rTRAIL induced apoptotic cell death in FLS in a dose-dependent manner. To clarify the functional role of DR4 and DR5 in TRAIL-mediated apoptosis in FLS, we performed the blocking experiments by the use of sDR4 and sDR5. sDR4 interferes with the interaction between TRAIL and DR4, and sDR5 interferes with that between TRAIL and DR5. As shown in Fig. 3, TRAIL-induced $\Delta\Psi$m in FLS was inhibited partially by sDR4 or sDR5, whereas it was inhibited completely by adding both sDR4 and sDR5. DR5 on FLS was suggested to be more functional to induce TRAIL-mediated apoptosis compared with DR4 (Fig. 3). In addition, OPG administration significantly suppressed TRAIL-mediated apoptosis in FLS (Fig. 3).

IL-1β-stimulated production of OPG by cultured FLS, which interferes with TRAIL-induced apoptogenic activity toward FLS

We examined the effects of inflammatory cytokines on OPG production by FLS. As shown in Fig. 4, OPG protein concentration increased time-dependently in the culture supernatants of FLS. Furthermore, such production was augmented by IL-1β at all time-points examined. Compared with IL-1β, the stimulatory effect of IL-6 (IL-6 + sIL-6 receptor) and TNF-α on OPG production from FLS was not found (data not shown). It was interesting to note that the rate of FLS apoptosis in response to TRAIL was decreased when rTRAIL was added without replacing the culture media (Fig. 5). Inhibition was more prominent in IL-1β-stimulated FLS compared with untreated FLS (Fig. 5), which was mainly restored by adding anti-OPG MoAb in culture media (Fig. 5). IL-1β treatment itself modulated neither TRAIL receptor expression (Fig. 6) nor TRAIL-mediated apoptosis (Fig. 5). These data suggest that OPG produced from FLS into the culture media is an endogenous receptor antagonist towards TRAIL-induced apoptosis of FLS.

DISCUSSION

Apoptosis occurs in a variety of physiological situations such as embryogenesis, and plays a crucial role in normal tissue homeostasis. However, a breakdown in the delicate balance between cell survival and apoptosis has been implicated in the pathogenesis of a number of rheumatic diseases, including RA [8]. The mechanisms responsible for synovial hyperplasia of RA patients may be explained by reduced synovial cell apoptosis, which cannot counteract the ongoing process of synovial cell proliferation.

TRAIL can interact potentially with five different receptors: two functional receptors DR4 and DR5, two decoy receptors DcR1 and DcR2, and a soluble decoy receptor OPG [12,17,18]. Other investigators have shown that DR5 is a sole death domain containing receptor for TRAIL on FLS [19]. We have shown here that DR5 was not sole but a prominent death domain-containing receptor for TRAIL. A previous study has shown that DR5 has the highest binding affinity towards TRAIL at 37°C [20];

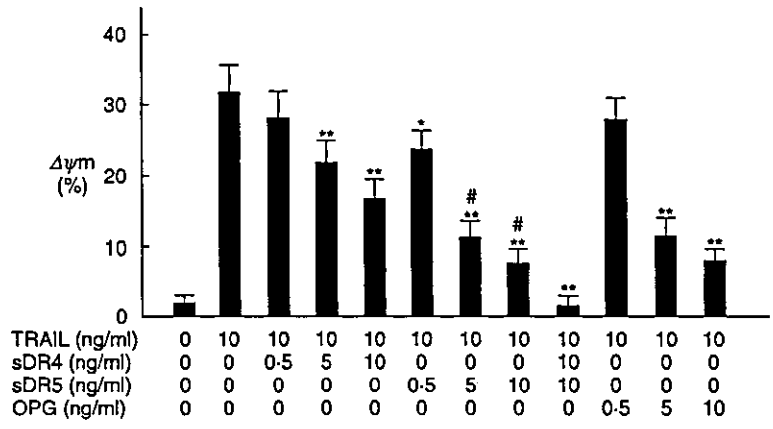

Fig. 3. Inhibition of TRAIL-mediated apoptosis in FLS by sDR4, sDR5 and OPG. FLS were cultured with 10 ng/ml of rTRAIL in the presence of varying concentrations of sDR4, SDR5 or OPG for 2 h. After incubation, apoptosis of FLS was quantified by $\Delta\Psi$m as described in the text. Note that TRAIL-mediated apoptosis in FLS was suppressed by sDR4, sDR5 and OPG; however, the inhibition was not complete. TRAIL-mediated apoptosis in FLS was inhibited completely by administration of both sDR4 and sDR5. $^*P < 0{\cdot}05$ *versus* FLS cultured with rTRAIL. $^{**}P < 0{\cdot}01$ *versus* FLS treated with rTRAIL. $\#P < 0{\cdot}05$ *versus* FLS treated with rTRAIL and sDR4. Data are the mean ± s.d. of four individual samples.

however, detailed experiments such as RNA interference for each TRAIL receptor are necessary to clarify the difference.

Recent studies reported the production of OPG in culture supernatants from rheumatoid FLS [16]. Thus, we focused on the regulatory role of inflammatory cytokines on OPG production by rheumatoid FLS. Our data suggest that OPG production in the rheumatoid microenviroment is, at least in part, positively regulated by IL-1β, which is consistent with recent observations by Ziokowska *et al.* [16]. The positive correlation between IL-6 and OPG protein concentration found in the rheumatoid synovial fluid may result from the inducible effect of IL-1β on the production of IL-6 [21], as the effect of IL-6 on OPG production by synovial cells was not found compared with IL-1β. A promising inhibitory role of OPG on osteoclastogenesis in murine adjuvant arthritis has been identified, which is achieved through decoy function of OPG for RANKL; however, treatment of the mice with OPG failed to improve the severity of synovial inflammation [22]. The present study has demonstrated that OPG is a functional inhibitor of TRAIL-induced apoptosis in FLS. Therefore, we speculate that the functional role of OPG on synovial cell growth is separate from its inhibitory action on osteoclastogenesis; the former is mediated through decoy function towards TRAIL while the latter through decoy function towards RANKL. Expression of TRAIL receptors on FLS was not affected by IL-1β treatment, and the sensitivity of TRAIL-mediated apoptosis was not suppressed directly by IL-1β; however, TRAIL-mediated apoptogenic activity towards FLS was inhibited significantly in IL-1β-stimulated FLS culture. The production of OPG from cultured FLS was augmented by IL-1β, thus IL-1β may inhibit primarily TRAIL-induced apoptosis of FLS at death receptor level by OPG in a competitive manner. This is consistent with data from the blocking experiment, that neutralization of OPG produced from FLS by anti-OPG MoAb mainly restored TRAIL-mediated apoptogenic activity towards FLS. Although OPG protein concentration in culture supernatants from IL-1β-treated synovial cells was comparable to that inhibiting TRAIL-induced FLS apoptosis (compare Figs 3 and 4), the concentration was clearly higher than that in the synovial fluid of RA patients (compare Fig. 1 with Figs 3 and 4), which could not suppress TRAIL-

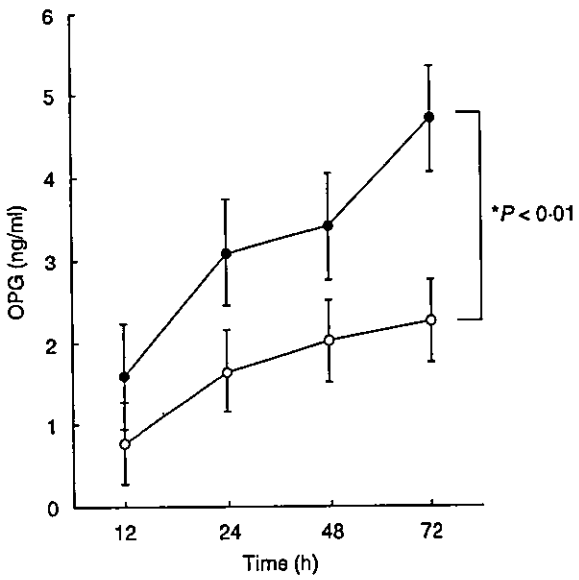

Fig. 4. IL-1β markedly stimulates OPG accumulation in culture supernatants of FLS. Rheumatoid FLS were cultured in the presence or absence of 20 IU/ml of IL-1β for indicated duration. After cultivation, OPG protein concentration in the culture supernatants was examined as described in the text. Open circles: unstimulated FLS, closed circles: IL-1β-treated FLS. *$P < 0{\cdot}01$ *versus* unstimulated FLS. Data are mean ± s.d. of seven individual samples.

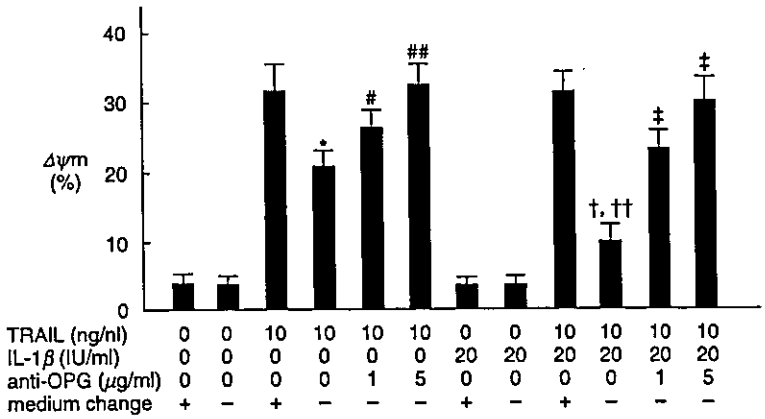

Fig. 5. OPG produced from FLS inhibits TRAIL-mediated apoptosis in FLS. FLS were cultured in the presence or absence of 20 IU/ml of IL-1β for 72 h with or without adding anti-OPG MoAb (1 μg/ml or 5 μg/ml). After cultivation, 10 ng/ml of rTRAIL was added to the culture with or without exchanging the culture media for an additional 2 h. After incubation, apoptosis of FLS was quantified by $\Delta\Psi$m as described in the text. Note that the sensitivity of FLS to TRAIL-mediated apoptosis was reduced when rTRAIL was added without exchanging the culture media, which was found significantly in IL-1β-treated FLS compared with unstimulated FLS. Furthermore, that inhibition was mainly restored by adding anti-OPG MoAb. Anti-OPG MoAb was mouse IgG1, thus 5 μg/ml of control mouse IgG1 (MBL) was used for negative control (0 μg/ml of anti-OPG MoAb means the addition of 5 μg/ml of control mouse IgG1). *$P < 0{\cdot}01$ *versus* unstimulated FLS treated with rTRAIL with exchanging culture media. #$P < 0{\cdot}05$. ##$P < 0{\cdot}01$ *versus* unstimulated FLS treated with rTRAIL without exchanging culture media. †$P < 0{\cdot}01$ *versus* IL-1β-stimulated FLS treated with rTRAIL with exchanging culture media. ††$P < 0{\cdot}05$ *versus* unstimulated FLS treated with rTRAIL without exchanging culture media. ‡$P < 0{\cdot}01$ *versus* IL-1β-stimulated FLS treated with rTRAIL without exchanging culture media. Data are the mean ± s.d. of four experiments.

